Electronic Supplementary Information

A Palindromic Triplex Architecture for DNA-Templated Synthesis Designed for the Core of a Synthetic Ribosome.

Rana Abdul Razzak[a,b], Jonathan Bath[a,b], Rachel K. O'Reilly[c], Andrew J. Turberfield[a,b]*

[a]University of Oxford, Department of Physics, Parks Road, Oxford OX1 3PU, United Kingdom.
[b]Kavli Institute for Nanoscience Discovery, South Parks Rd, Oxford, OX1 3QU, United Kingdom.
[c]School of Chemistry, University of Birmingham, Edgbaston, Birmingham, B15 2TT United Kingdom

Table of Contents

1. Abbreviations

MOPS: (3-(N-morpholino)propanesulfonic acid)

PAGE: Polyacrylamide gel electrophoresis

EDTA: Ethylenediaminetetraacetic acid

BPB: Bromophenol blue

DMT-MM: 4-(4,6-Dimethoxy-1,3,5-triazin-2-yl)-4-methylmorpholinium chloride

TCEP.HCl: Tris(2-carboxyethyl)phosphine hydrochloride

DBCO: Dibenzocyclooctyne

DNA: Deoxyribonucleic acid

W-C: Watson-Crick interactions

R.H: Reversed Hoogsteen

dsDNA: Double-stranded DNA

ssDNA: Single-stranded DNA

DTS: DNA-templated synthesis

FRET: Förster resonance energy transfer

FWHM: Full width at half maximum

T: Template

T^C: Template-complement

T*: Mismatched template (mismatched to adapter oligos in triplex-forming domain)

T^C*: Mismatched template-complement (complementary to T*)

Temp.: Temperature

Prod.: Product

NTC: Non-templated control

bp: base pair

^{1}H NMR: Proton nuclear magnetic resonance

^{13}C NMR: Carbon-13 nuclear magnetic resonance

DMSO-d6: Deuterated dimethyl sulfoxide

δ: Chemical shift in parts per million (ppm)

s: Singlet

t: Triplet

m: Multiplet

2. Supporting Methods

2.1. General Experimental Materials and Instrumentation

Unless otherwise stated, chemical reagents were purchased at the highest commercial quality and used without further purification. Non-modified DNA oligonucleotides were purchased from Integrated DNA Technologies, B.V. Modified DNA oligonucleotides were purchased from Biomers.net GmbH. Restriction enzymes (AvaI and SacI-HF®) were purchased from New England Biolabs. Water in all reactions was purified by a Millipore Milli-Q water filtration system. All gels were cast with a BIORAD Mini-PROTEAN Gel Kit, run with a BIORAD PowerPac Basic Power Supply and imaged with an GE Amersham Typhoon FLA9500 gel scanner. SYBR™ Gold nucleic acid gel stain was obtained from ThermoFisher Scientific. Samples were annealed or incubated at specific temperatures using an Eppendorf Mastercycler nexus thermocycler.

2.2. Annealing Protocol I

Oligonucleotides were annealed by heating to 99 ºC then cooling to 24 ºC at a rate of 1 ºC/minute.

2.3. Annealing Protocol II

Oligonucleotides were annealed by heating to 99 ºC then cooling to 24 ºC at a rate of 0.3 ºC/minute.

2.4. Restriction Endonuclease Protection (Figure S3)

Restriction endonuclease protection assay was performed as described previously.[36] The adjacent inverted purine tracts in the dsDNA were designed to overlap a six base-pair sequence that is recognised and cut by a restriction endonuclease (5′-CTCGAG-3′ recognised by AvaI and 5′-GAGCTC-3′ recognised by SacI-HF®). DNA template, T (1.00 equiv., 100 nM), complementary strand, T^C (1.08 equiv., 108 nM), and DNA adapters, A1 (1.09 equiv., 109 nM) and A_2 (1.09 equiv., 109 nM), were annealed (protocol I) in MOPS buffer (25 mM, pH 7.7) supplemented with $MgCl_2$ (20 mM) and NaCl (70 mM) in a reaction volume of 32 µL (concentrations specified are final concentrations in this 32 µL reaction mixture). After annealing, the complexes were equilibrated at 24 ºC overnight, then the restriction endonuclease (10 units) was added, and the reaction was incubated at 37 ºC for 3 hrs. The digestion was terminated by addition of EDTA (0.5 M, 10 µL, pH 8.0). A sample (3.1 µL) of the reaction mixture was removed, mixed with a denaturing loading buffer (17.9 µL, 94% formamide, 6% BPB) and heated at 60 ºC for 15 min. DNA fragments were analysed by denaturing PAGE (14% gel containing 47% acrylamide: bis-acrylamide (30%, 19:1), 17%

formamide, 3% TBE (10×) and 47% W/V urea). The gel was run with 1× TBE running buffer at 300V for 60 min at room temperature. Bands were visualised by gel staining using SYBR™ Gold and scanned using an Amersham™ Typhoon™ Biomolecular Imager (excitation laser 488 nm, emission filter name=Cy2 525BP20). Gel images were analysed using ImageJ.

Sequences used (supporting figures, Figure S3)**:**

For 3′-3′ T3′, T*3′, T^C3′, T^C*3′, A1-3′, and A2-3′

For 5′-5′ T5′, T*5′, T^C5′, T^C*5′, A1-5′, and A2-5′

2.5. FRET Melting Assay (Figures S4 and S5)

To observe the melting of the templating complex by FRET spectroscopy, the two adapter oligos, A1 and A2, were labelled at their 3′-ends (for sequences juxtaposing 3′ ends) or at their 5′-ends (for sequences juxtaposing 5′ ends), with cyanine 3 (Cy3) as the donor and cyanine 5 (Cy5) as the acceptor, respectively. DNA template T (1.00 equiv., 100 nM), complementary strand, T^C (1.08 equiv., 108 nM), and DNA adapters, A1-Cy3 (1.09 equiv., 109 nM) and A2-Cy5 (1.09 equiv., 109 nM) were annealed (protocol II) in MOPS buffer (25 mM, pH 7.7) supplemented with $MgCl_2$ (20 mM) and NaCl (70 mM) in a reaction volume of 32 µL (concentrations are specified as final concentrations in this reaction mixture). After annealing, the complexes were equilibrated at 24 ºC overnight. Melting of the preassembled complexes was monitored using a real-time PCR apparatus (Stratagene Mx3005P).[37,38] Three filter sets were used. With the Cy3 filter set, Cy3 was excited at 535 nm and its emission recorded at 568 nm. With the Cy5 filter set, Cy5 was excited at 635 nm and its emission recorded at 665 nm. With the FRET filter set, Cy3 was excited at 535 nm and Cy5 emission was recorded at 665 nm. FWHM of all filters was 10 nm. The variation of emission intensities with temperature was monitored in the range between 25 and 80 ºC. Heating and cooling were carried out at a rate of 0.3 ºC/minute. Measurements were repeated three times and then averaged. Determination of melting transitions is complicated by temperature-induced quenching of both Cy3 and Cy5 emission and by sequence- and assembly-dependent interactions between the dyes and neighbouring nucleobases.[39-42] To enhance the clarity of the melting transition, the Cy5 emission signal obtained through the FRET filter set (excitation at 535 nm and emission at 665 nm) was divided by the Cy5 emission signal obtained through direct excitation (excitation at 635 nm and emission at 665 nm).[43-45] The resulting ratio was then plotted against temperature. The upper (I_U) and lower (I_L) baselines were determined by using linear regression to fit linear regions before and after the melting transition.[46] The intercept of the algebraic mean of the two baselines with the curve was taken as a measure of the melting temperature.[46] The assembled fraction θ at temperature T was approximated using equation (1).

$$\theta(T) = \frac{I_{FRET}(T) - I_L(T)}{I_U(T) - I_L(T)} \quad (1)$$

The melting temperature corresponds to $\theta = 0.5$.

Sequences used (supporting figures, Figures S4 and S5)**:**

For 3′-3′ T3′, T*3′, T^C3′, T^C*3′, A1-3′-Cy3, and A2-3′-Cy5

For 5′-5′ T5′, T*5′, T^C5′, T^C*5′, A1-5′-Cy3, and A2-5′-Cy5

2.6. DNA-Templated Amide-Bond Formation (Figure 2)

DNA template T (1.00 equiv., 100 nm), complementary strand T^C (1.08 equiv., 108 nM), and DNA adapters A1-NH_2 (1.09 equiv., 109 nM) and A2-COOH (1.09 equiv., 109 nM) were annealed (using annealing protocol I) in MOPS buffer (25 mM, pH 7.7) supplemented with $MgCl_2$ (20 mM) and in a reaction volume of 32 µL (concentrations are specified as final concentrations in this reaction mixture). After annealing, the complexes were equilibrated at 24 ºC overnight. DMT-MM (3.2 µL, 500 mM) was added, bringing the volume to 35.2 µL and concentrations to: DNA template T 91 nM, complementary strand T^C 98 nM, and DNA adapters A1-NH_2 and A2-COOH 99 nM each, MOPS buffer 23 mM (pH 7.7), DMT-MM 45 mM, $MgCl_2$ 18 mM. The reaction was allowed to proceed overnight at 25 ºC. A sample (2.7 µL) of the reaction mixture was removed for analysis, mixed with a denaturing loading buffer (17.5 µL, 94% formamide, 6% BPB) and heated at 60 ºC for 15 min. Reaction products were analysed by denaturing PAGE (14% gel containing 47% acrylamide:bis-acrylamide (30%, 19:1), 17% formamide, 3% TBE (10×) and 47% W/V urea). The gel was run with 1×TBE buffer at 300V for 60 min at room temperature. Bands were visualised by staining using SYBR™ Gold then scanning using an Amersham™ Typhoon™ Biomolecular Imager (excitation laser 488 nm, emission filter name=Cy2 525BP20). Gel images were analysed using ImageJ. Yields were approximated by:

$$Yield\% = \frac{I_{A1-A2}}{I_{A1-A2} + I_{A1-NH_2} + I_{A2-COOH}} \times 100 \quad (2)$$

where I_{A1-A2} is the intensity of the band corresponding to the product of adapters A1 and A2's ligation, and I_{A1-NH_2} and $I_{A2-COOH}$ are the intensities of bands corresponding to A1-NH_2 and A2-COOH, respectively. Note that the templated reaction yield was limited by the concentration of the template to 92%.

Sequences used (main text, Figure 2)

For 3′-3′ T3′, T*3′, T^C3′, T^C*3′, A1-3′-AminoC_6, and A2-3′-COOH

For 5′-5′ T5′, T*5′, T^C5′, T^C*5′, A1-5′-AminoC_5, and A2-5′-COOH

2.7. DNA-Templated Copper-Free Click (Figure 3)

DNA template T (1.00 equiv., 100 nM) and complementary strand T^C (1.08 equiv., 108 nM) were annealed (protocol I) in MOPS buffer (25 mM, pH 7.7) supplemented with $MgCl_2$ (20 mM). After annealing, the complexes were equilibrated at 24 ºC for one hour, then A1-DBCO (1.09 equiv., 109 nM) was added and allowed to assemble at 45 ºC for one hour. A2-Azidobenzoate (1.09 equiv., 109 nM) was then added at 45 ºC bringing the reaction volume to 32 µL (concentrations are specified as final concentrations in the reaction mixture). The reaction mixture was left at 45 ºC for the designated period before the reaction was terminated by adding a solution of 6-azidohexanoic acid in formamide (10 µL, 335 mM). Reaction products were analysed by denaturing PAGE as described above.

Sequences used (main text, Figure 3)**:**

For 3′-3′ T3′, T*3′, T^C3′, T^C*3′, A1-3′-DBCO, and A2-3′-Azidobenzoate

For 5′-5′ T5′, T*5′, T^C5′, T^C*5′, A1-5′-DBCO, and A2-5′-Azidobenzoate

2.8. DNA-Templated Thiazolidine Synthesis (Figure 4)

DNA template T (1.00 equiv., 100 nM), complementary strand T^C (1.08 equiv., 108 nM), and DNA adapters A1-Benzaldehyde (1.09 equiv., 109 nM) and tert-butylthio protected A2-Cysteine (1.09 equiv., 109 nM) were annealed (protocol I) in MOPS buffer (25 mM, pH 7.7) supplemented with $MgCl_2$ (20 mM) in a reaction volume of 32 µL (concentrations are specified as final concentrations in the reaction mixture). After annealing, the complexes were equilibrated at 24 ºC overnight. TCEP.HCl (3.2 µL, 60 mM) was then added to deprotect the tert-butylthio protected A2-Cysteine, bringing the final volume to 35.2 µL and concentrations to: DNA template T 91 nM, complementary strand T^C 98 nM, and DNA adapters A1-3′-Benzaldehyde and tert-butylthio protected A2-3′-Cysteine 99 nM each, MOPS buffer 23 mM (pH 7.7), $MgCl_2$ 18 mM, TCEP.HCl 5.5 mM. The reaction mixture was run at 45 ºC for the designated period before the reaction was terminated by adding a solution of 4-hydroxybenzaldehyde in formamide (10 µL, 335 mM). Reaction products were analysed by denaturing PAGE as described above.

Sequences used (main text, Figure 4)**:**

For 3′-3′ T3′, T^C3′, A1-3′-Benzaldehyde, and tert-butylthio protected A2-3′-Cysteine

For 5′-5′ T5′, T^C5′, A1-5′-Benzaldehyde, and tert-butylthio protected A2-5′-Cysteine

2.9. DNA-Templated Amide-Bond Formation at Different Temperatures (Figure S9)

DNA oligos were annealed and equilibrated as described for “DNA-Templated Amide-Bond Formation (Figure 2)”. DMT-MM (3.2 µL, 500 mM) was added, and the reaction was allowed to

proceed overnight at the specified temperature (35-55 ºC). Conditions (concentrations are specified as final concentrations in the 35.2 µL reaction mixture): DNA template T 91 nM, complementary strand T^C 98 nM, and DNA adapters A1-NH_2 and A2-COOH 99 nM each, MOPS buffer 23 mM (pH 7.7), DMT-MM 45 mM, $MgCl_2$ 18 mM and NaCl 63.6 mM.

Sequences used (supporting figures, Figure S9):

For 3′-3′ T3′, T*3′, T^C3′, T^C*3′, A1-3′-AminoC_{12}, and A2-3′-COOH

For 5′-5′ T5′, T*5′, T^C5′, T^C*5′, A1-5′-AminoC_{12}, and A2-5′-COOH

For 3′-5′ (ATN) T3′, A1-3′- AminoC_{12}^{ATN}, and A1-5′- $COOH^{ATN}$

For 3′-3′ (NTC) A1-3′-AminoC_{12}, and A2-3′-COOH

2.10. DNA-Templated Amide-Bond Formation with Different Salt Concentrations (Figures S10-S13)

DNA oligos were annealed and equilibrated as described for "DNA-Templated Amide-Bond Formation (Figure 2)". DMT-MM (3.2 µL, 500 mM) was added, and the reaction was allowed to proceed overnight at the specified temperature (25 or 55 ºC). Conditions (concentrations are specified as final concentrations in the 35.2 µL reaction mixture): DNA template T 91 nM, complementary strand T^C 98 nM, and DNA adapters A1-NH_2 and A2-COOH 99 nM each, MOPS buffer 23 mM (pH 7.7), DMT-MM 45 mM, $MgCl_2$ 0-27.3 mM and NaCl 0-190.9 mM.

Sequences used (supporting figures, Figures S10-S13)

For 3′-3′ T3′, T*3′, T^C3′, T^C*3′, A1-3′-AminoC_{12}, and A2-3′-COOH

For 5′-5′ T5′, T*5′, T^C5′, T^C*5′, A1-5′-AminoC_{12}, and A2-5′-COOH

2.11. Effect of intervening base pairs on DNA-Templated Amide-Bond Formation (Figure S14)

This experiment was conducted using the protocol as described above for "DNA-Templated Amide-Bond Formation (Figure 2)".

Sequences used (supporting figures, Figure S14)**:**

For 3′-3′ T3′, T*3′, T^C3′, T^C*3′, T3′- $bp^{Intervening}$ =2-8, T^C3′-$bp^{Intervening}$ =2-8, T*3′- $bp^{Intervening}$ =2-8, T^C*3′- $bp^{Intervening}$ =2-8, A1-3′-AminoC_{12}, and A2-3′-COOH

For 5′-5′ T5′, T*5′, T^C5′, T^C*5′, T5′- $bp^{Intervening}$ =2-8, T^C5′- $bp^{Intervening}$ =2-8, T*5′- $bp^{Intervening}$ =2-8, T^C*5′- $bp^{Intervening}$ =2-8, A1-5′-AminoC_{12}, and A2-5′-COOH

2.12. Synthesis of 6-Azidohexanoic Acid

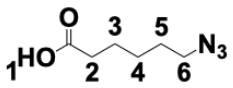

This compound was synthesized according to a literature procedure.[47] A round bottom flask (100 mL) was charged with 6-bromohexanoic acid (1.00 equiv., 4.00 g, 21 mmol), DMF (50 mL), and NaN_3 (1.05 equiv., 1.40 g, 22 mmol). The slurry was heated overnight at 40 ºC. Then, reaction mixture was diluted with ethyl acetate (50 mL) then filtered. The filtrate was washed with dilute HCl (0.1 M, 5×30 mL). The organic fraction was dried over sodium sulphate. Solvents were removed under reduced pressure to afford the desired product as a colourless oil (2.84 g, yield: 88%). ^{1}H NMR (750 MHz, DMSO-d6) δ 12.00 (s, 1H, 1), 3.31 (t, J = 6.87 Hz, 2H, 6), 2.21 (t, J = 7.35 Hz, 2H, 2), 1.56 – 1.47 (m, 4H, 3, 5), 1.36 – 1.29 (m, 2H, 4). ^{13}C NMR (189 MHz, DMSO-d6) δ 174.36, 50.51, 33.51, 27.99, 25.71, 24.02.

2.13. Model Building of Adjacent and Inverted (Palindromic) DNA Triplexes (Figure S15)

The palindromic triplex domain was modelled as described previously using Maestro version 12.9.123 from Schrödinger.[48,49] Initially, half of the palindromic DNA triplex was created using the 3D-NuS web server.[50] This triplex structure was duplicated, and the duplicate was rotated by 180º about an axis perpendicular to the helix axis. The two triple helices were docked so that the purine strand of the W.C duplex of one triplex model would form a 5′-3′ internucleotide junction with the pyrimidine strand of the W.C duplex of the other triplex model. This juxtaposes the 3′-3′ ends of the two triplex-forming strands. The 5′-3′ internucleotide junctions were subsequently connected via phosphate diester linkages. Finally, the strands were renamed and residues renumbered. The complex juxtaposing 5′-5′ ends was built similarly. Steric clashes were removed and the energy of the system minimized using Gromacs (release 2020.4).[51] The system was prepared using the Charmm27 force field and solvated in a cubic box with 62 magnesium ions (Mg^{2+}), 62 chloride ions (Cl^-) and 29099 water molecules modelled by the TIP3P water model.[52-54] Energy minimization was performed using the steepest descent algorithm, with a convergence criterion of a maximum force tolerance (Fmax) of less than 1000 kJ/mol/nm. 3D models and base-stacking diagrams were produced using UCSF Chimera version 1.15.[55]

3. Supporting Figures

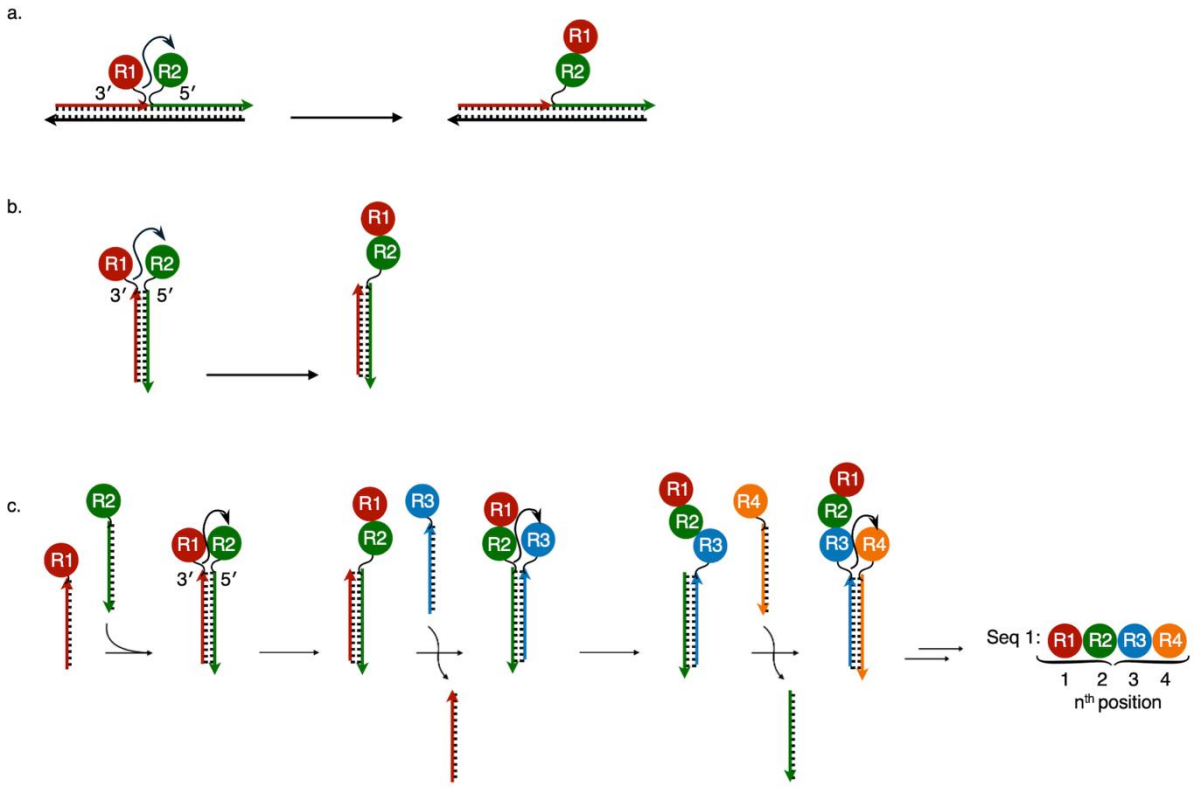

3.1. Figure S1. Commonly-used reaction geometries for DNA-templated synthesis.

a) Across-the-nick; b) end-of-helix. In both cases the reaction occurs between a building block conjugated to the 3′ end of its adapter and one at the 5′ end. c) Schematic of oligomer synthesis by a programmed sequence of end-of-helix transfer reactions involving alternately 3′- and 5′- conjugated building blocks. Details of the mechanisms for sequential removal and replacement of spent adapters are omitted.

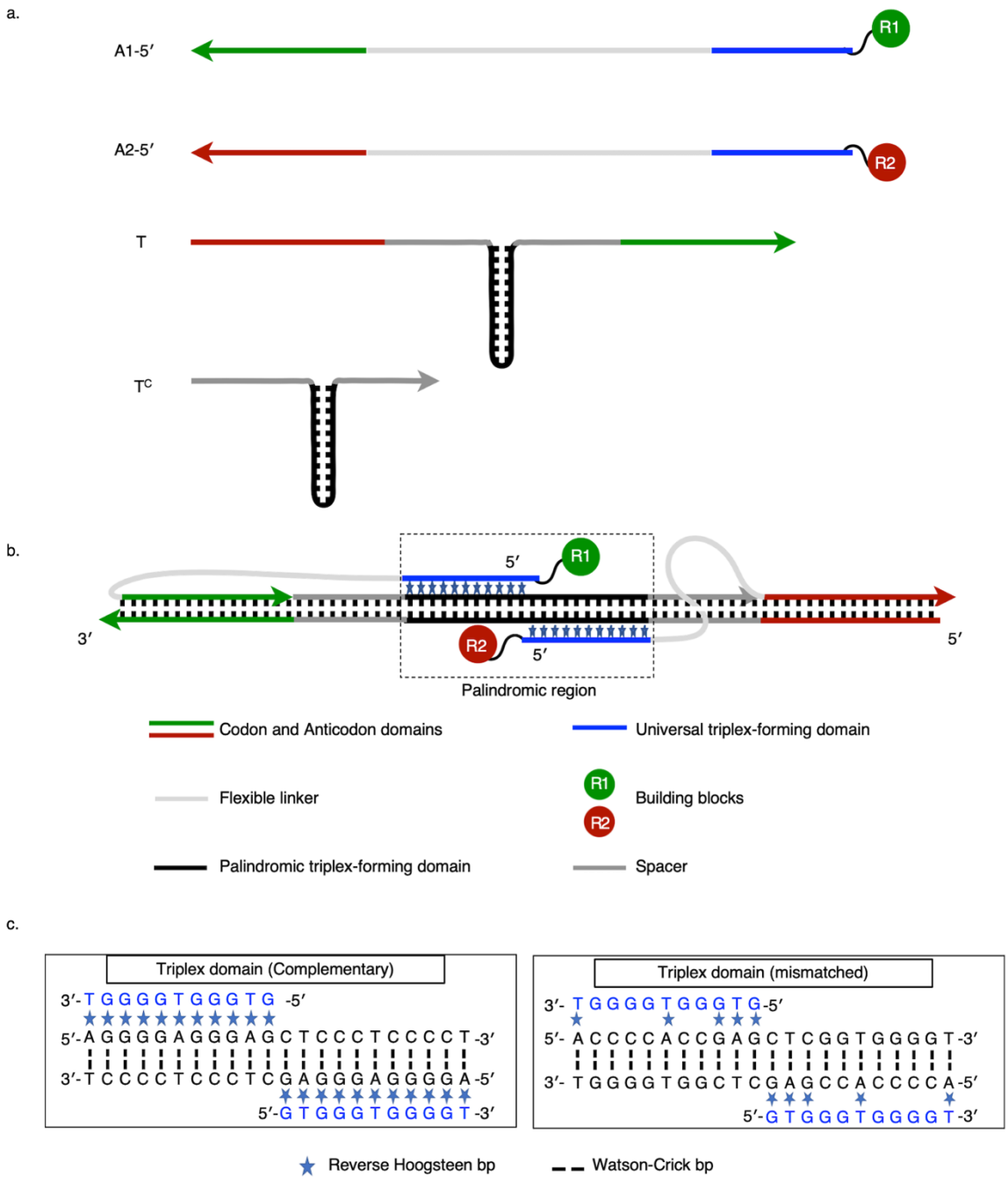

3.2. Figure S2. The triplex template juxtaposing 5'-conjugated building blocks.

(a) Components: two DNA adapters (A1 and A2), the templating gene (T) and its partial complement (T^C). Each adapter comprises an identifying anticodon domain separated by a flexible linker from a universal triplex-forming domain adjacent to the conjugated building block. The adapters are identical except for their reactive building blocks and the corresponding anticodon domains. The palindromic central sections of T and T^C comprise polypurine and polypyrimidine domains. (b) T and T^C form a templating duplex (dsDNA) with adjacent, inverted, triplex-forming domains, formed by hybridization of the palindromic sections, and overhanging ssDNA codons. A1 and A2 bind to the template through their (distinct) anticodon and (identical) triplex-forming domains (c). Triplexes formed by the 5' ends of the adapters and the palindromic central section of the template duplex bring the 5′ ends of A1 and A2 into proximity. (c) Base sequences of complementary and mismatched templating triplex domains.

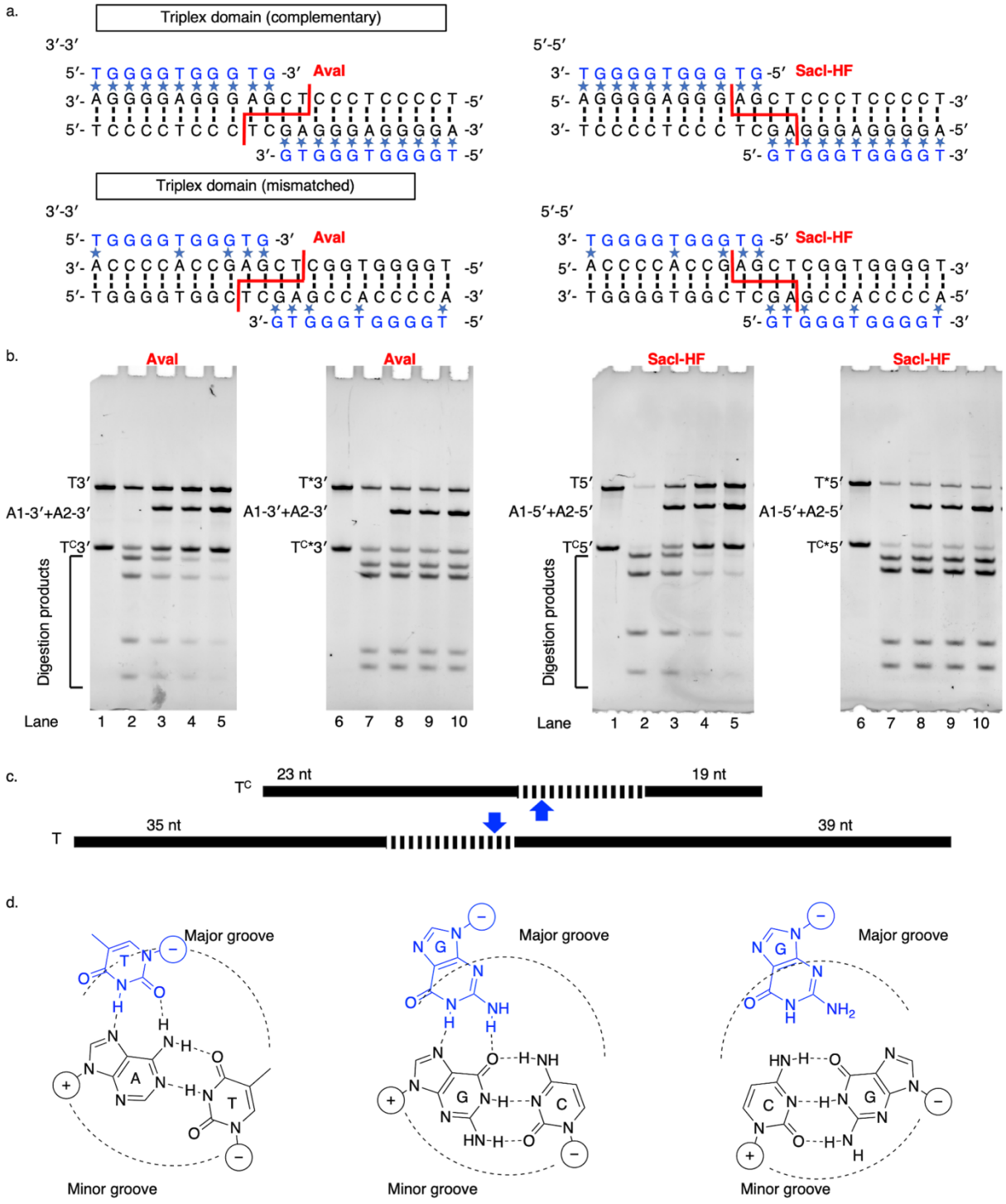

3.3. Figure S3. Restriction endonuclease protection assay.

(a) Sequences of the triplex domains juxtaposing 3′-3′ and 5′-5′ termini. The 6-bp AvaI and SacI-HF restriction sites, respectively, are indicated. (b) Denaturing PAGE of digestion products of sequences juxtaposing 3′-3′ by AvaI (left) and 5′-5′ by SacI-HF (right). The asterisk denotes the triplex-mismatched sequence (right-hand gel of each pair). Lanes: 1 and 6, undigested dsDNA; 2 and 7, digested dsDNA without adapters; 3 and 8, digestion in the presence of A1; 4 and 9, digestion in the presence of A2; 5 and 10, digestion in the presence of A1&A2. Conditions: DNA strands T, T^C, A1 and A2 were annealed in MOPS buffer (pH 7.7) with $MgCl_2$ and NaCl (final concentrations: 100 nM T, 108 nM T^C, 109 nM A1, 109 nM A2, 25 mM MOPS, 20 mM $MgCl_2$ and 70 mM NaCl in a total volume of 32 µL). Complexes were equilibrated for 20 hrs at 24 ºC before the addition of enzyme (10 units) and incubation at 37 ºC for 3 hours. Digestion was terminated

by EDTA addition, and the reaction was analysed by 14% denaturing PAGE. (c) Restriction maps. Arrows indicate the restriction sites, and hashed rectangles indicate triplex domains. Restriction of dsDNA yields four fragments of 39, 35, 23, and 19 nucleotides. (d) Base triplets used in this study. Plus and minus signs denote relative strand polarities. G opposite CG does not form hydrogen bonds and is therefore a mismatched triplex base. For more details see "2.4. Restriction Endonuclease Protection" in the methods section. Sequences used in this experiment are**:** (For 3′-3′) T3′, T*3′, T^{C}3′, T^{C}*3′, A1-3′, and A2-3′. (For 5′-5′) T5′, T*5′, T^{C}5′, T^{C}*5′, A1-5′, and A2-5′.

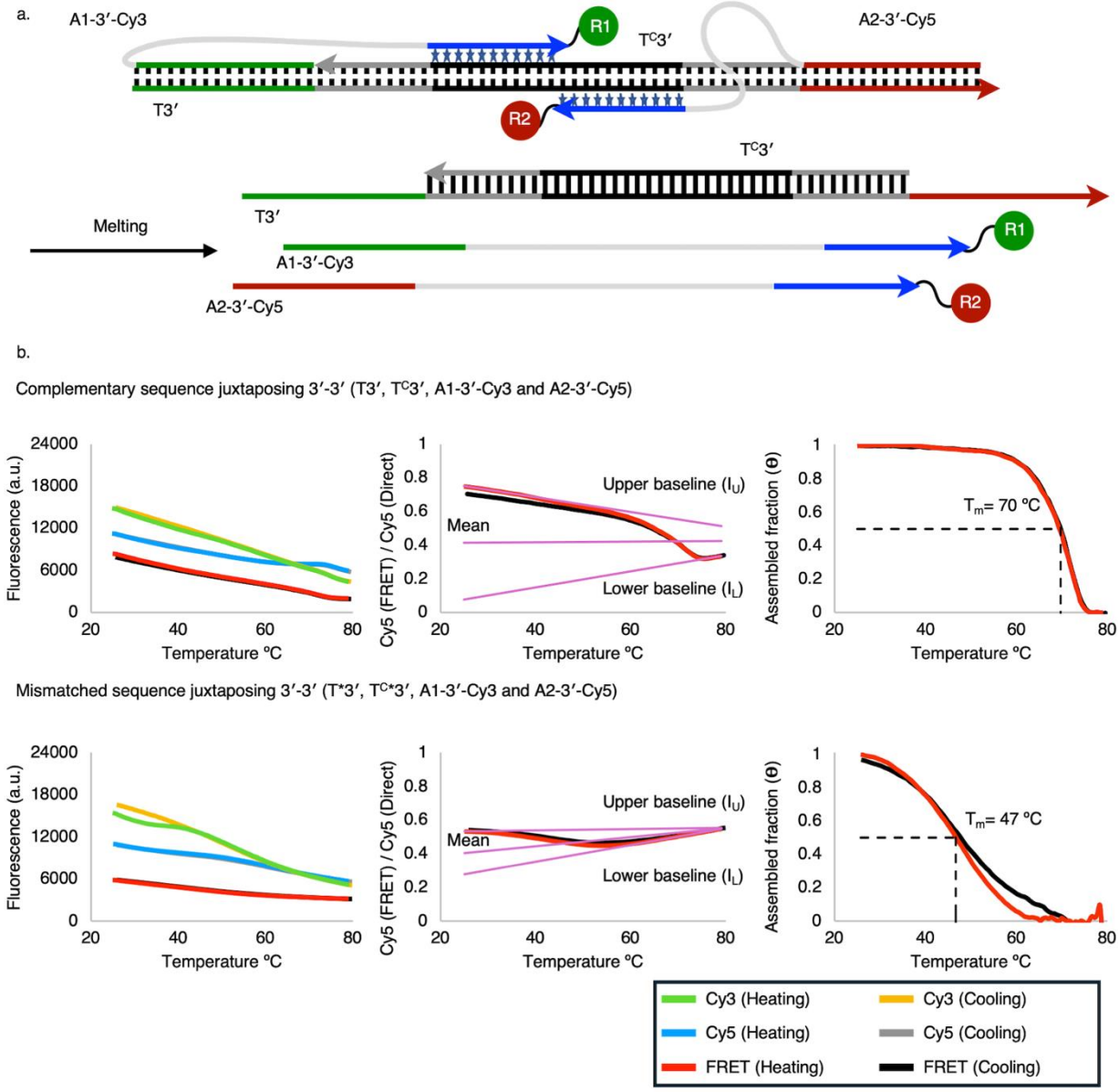

3.4. Figure S4. FRET melting assay: 3′ modifications.

Schematic representation of the FRET melting assay performed using sequences juxtaposing 3′-3′ ends. Base sequences of complementary and mismatched triplex-forming domains are shown in Figure 1. (b) Fluorescence intensities (left), fitted baselines (centre) and corresponding assembled fractions (right panels, see Supporting methods) as functions of temperature. (The calculated melting temperature of the central T- T^C duplex is 95 ºC.) Conditions: DNA strands T, T^C, A1-3′-Cy3 and A2-3′-Cy5 were annealed in MOPS buffer (pH 7.7) with $MgCl_2$ and NaCl (final concentrations: 100 nM T, 108 nM T^C, 109 nM A1, 109 nM A2, 25 mM MOPS, 20 mM $MgCl_2$ and 70 mM NaCl in a total volume of 32 µL). Following annealing, complexes were equilibrated at 24 ºC for 20 hrs. Melting was monitored using a Stratagene Mx3005P real-time PCR with three filter sets: Cy3 (excitation at 535 nm, emission at 568 nm), Cy5 (excitation at 635 nm, emission at 665 nm), and FRET (Cy3 excitation at 535 nm, Cy5 emission at 665 nm). Emission intensity was recorded from 25 to 80 ºC at a heating/cooling rate of 0.3 ºC/min. Measurements were taken in triplicate and averaged. For more details, see "2.5. FRET Melting Assay" in the methods section. Determination of melting transitions is complicated by temperature-induced quenching of both Cy3 and Cy5 emission and by sequence- and assembly-dependent interactions between the dyes and neighbouring nucleobases. Nevertheless, it is clear that the melting

transition with a fully-matched triplex sequence is sharper and occurs at higher temperature than that corresponding to the mismatched sequence. The assumption that the assembled fraction can be determined by the deviation of the FRET signal from the fitted baselines (see Methods) provides an approximate quantification of the melting transition.

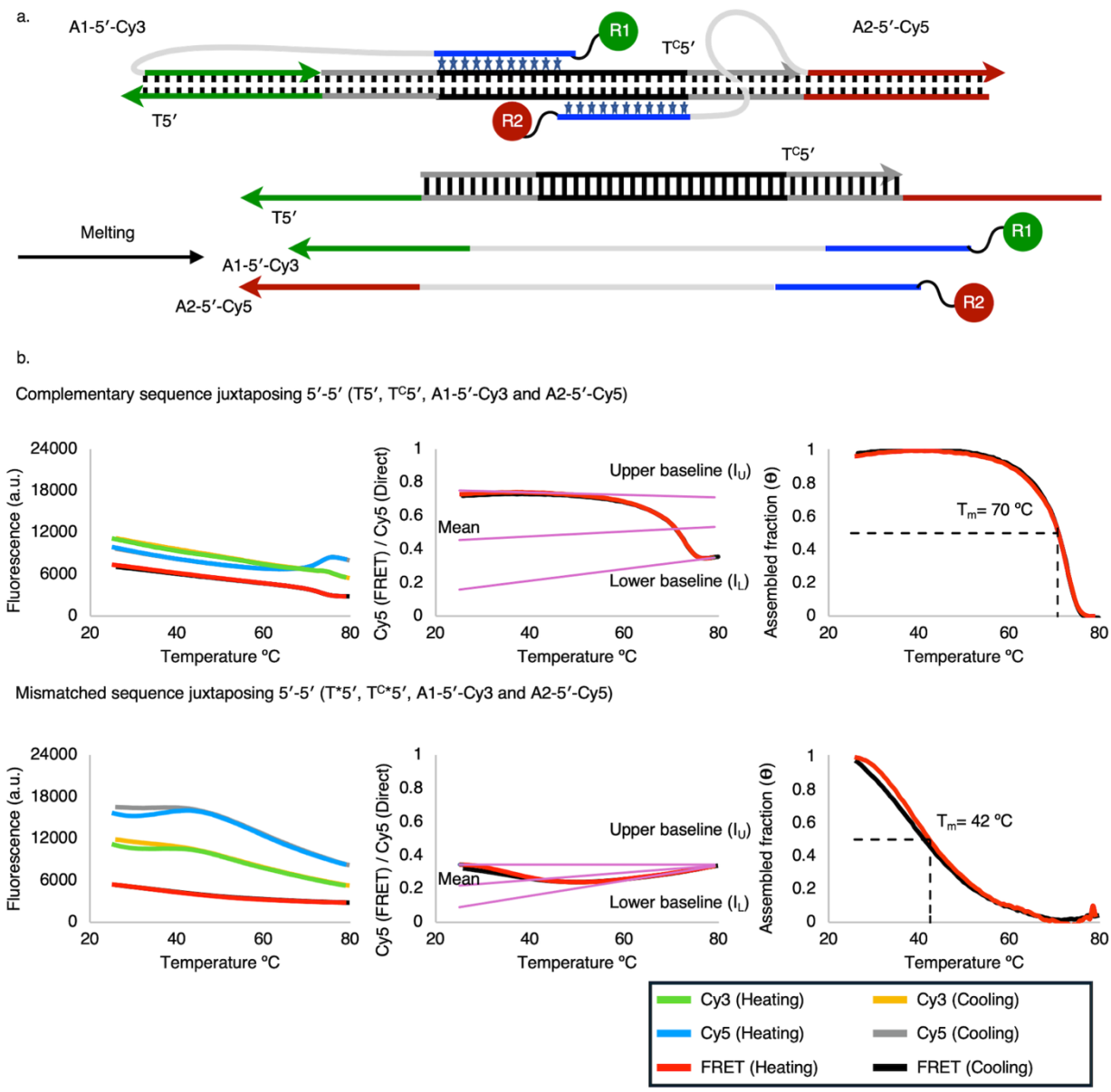

3.5. Figure S5. FRET melting assay: 5′ modifications.

(a) Schematic representation of the FRET melting assay performed using sequences juxtaposing 5′-5′ ends. Base sequences of complementary and mismatched triplex-forming domains are shown in Figure S2. (b) Fluorescence intensities (left), fitted baselines (centre) and corresponding assembled fractions (right panels, see Supporting methods) as functions of temperature. (The calculated melting temperature of the central T- T^C duplex is 95 ºC.) Conditions: DNA strands T, T^C, A1-3′-Cy3 and A2-5′-Cy5 were annealed in MOPS buffer (pH 7.7) with $MgCl_2$ and NaCl (final concentrations: 100 nM T, 108 nM T^C, 109 nM A1, 109 nM A2, 25 mM MOPS, 20 mM $MgCl_2$ and 70 mM NaCl in a total volume of 32 µL). Following annealing, complexes were equilibrated at 24 ºC for 20 hrs. Melting was monitored using a Stratagene Mx3005P real-time PCR with three filter sets: Cy3 (excitation at 535 nm, emission at 568 nm), Cy5 (excitation at 635 nm, emission at 665 nm), and FRET (Cy3 excitation at 535 nm, Cy5 emission at 665 nm). Emission intensity was recorded from 25 to 80 ºC at a heating/cooling rate of 0.3 ºC/min. Measurements were taken in triplicate and averaged. For more details, see "2.5. FRET Melting Assay" in the methods section and comments in caption to Figure S4.

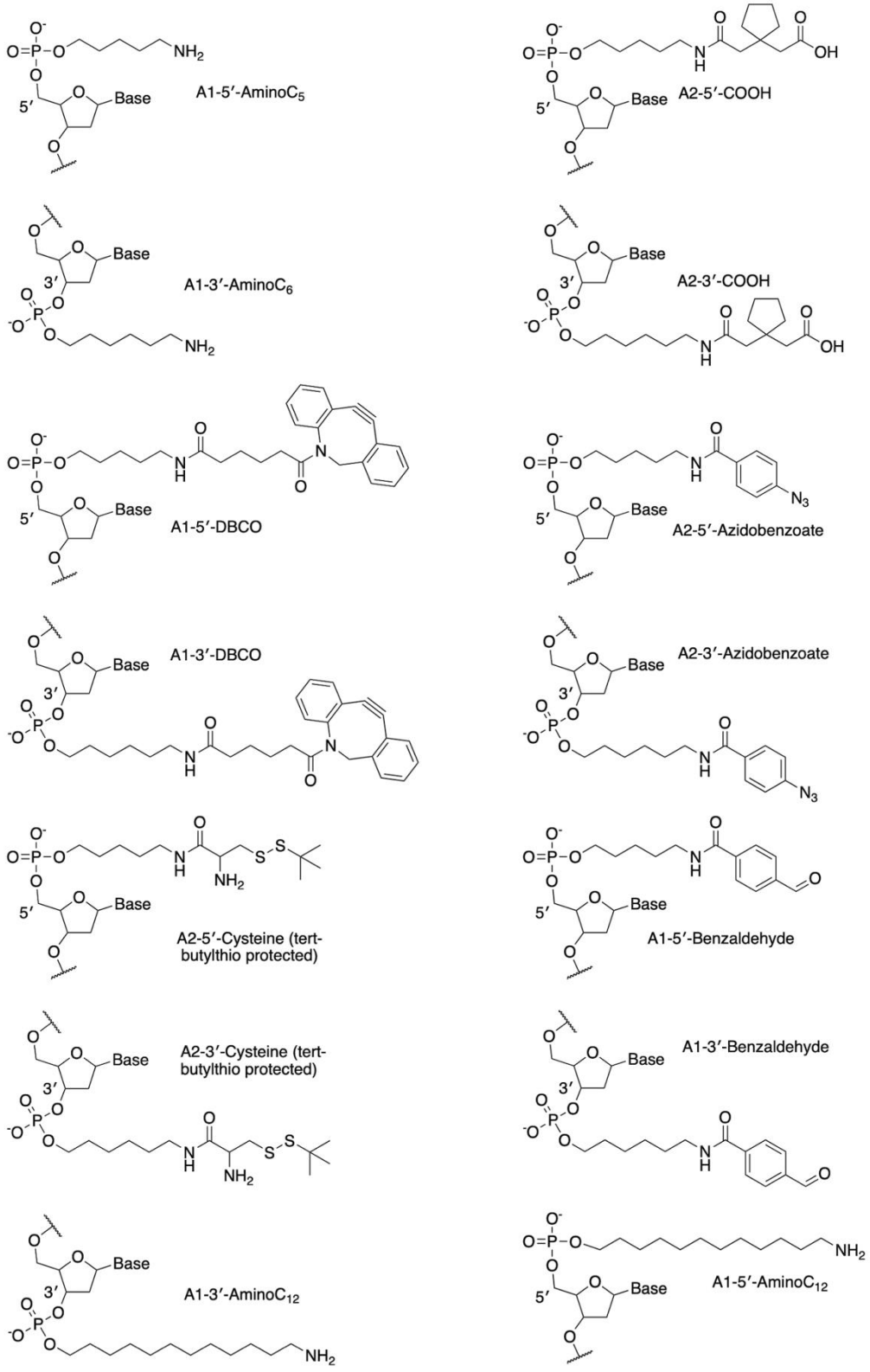

3.6. Figure S6. Structures of 3′ and 5′ modifications used in this work.

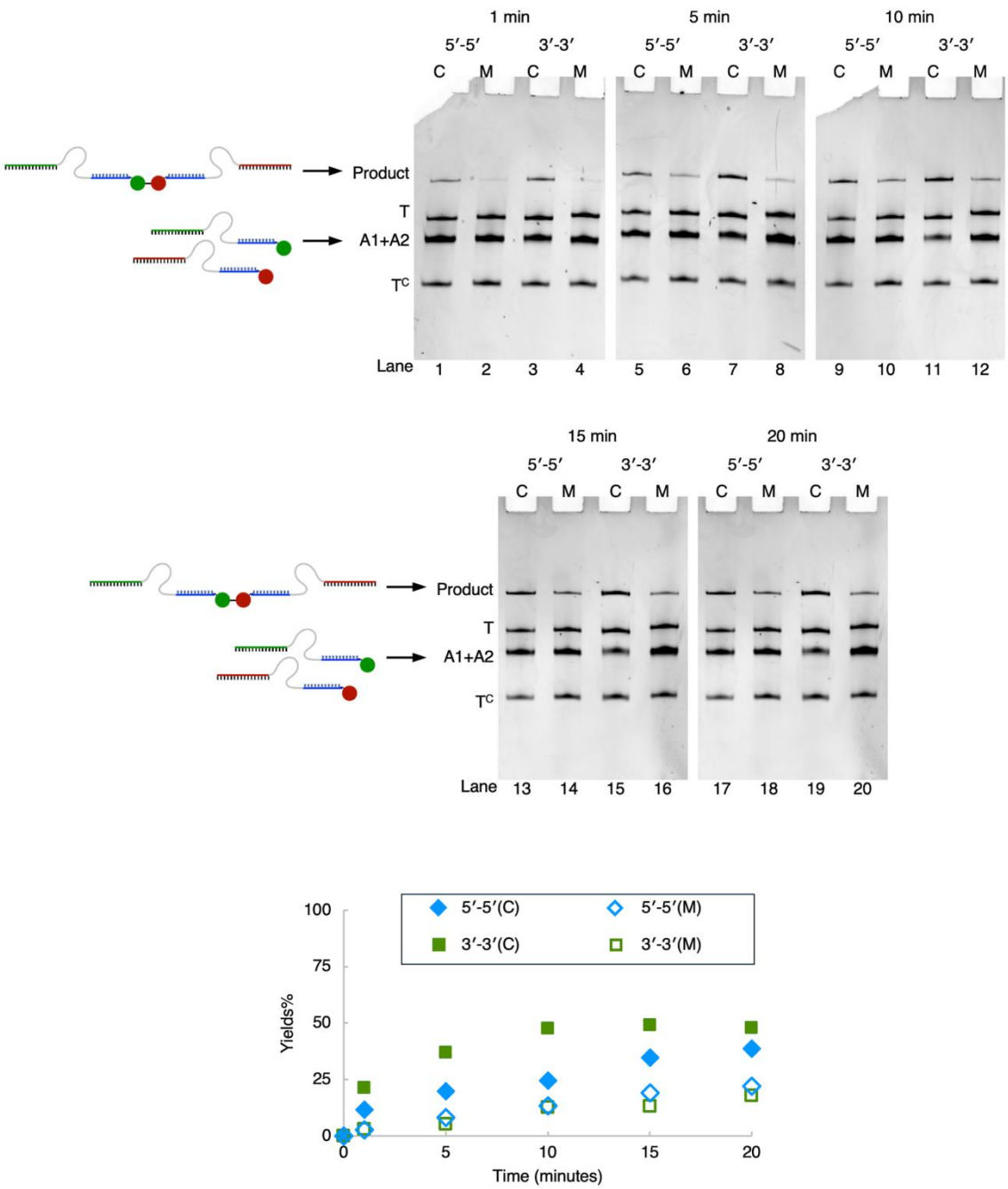

3.7. Figure S7. Denaturing PAGE analysis of DNA-templated copper-free click conjugation.

Templated copper-free click between 3′-conjugated reactants is faster than between 5′-conjugated reactants. For more details, see “2.7. DNA-Templated Copper-Free Click” in the methods section. Sequences used in this experiment are: (For 3′-3′) T3′, T*3′, TC3′, TC*3′, A1-3′-DBCO, and A2-3′-Azidobenzoate. (For 5′-5′) T5′, T*5′, TC5′, TC*5′, A1-5′-DBCO and A2-5′-Azidobenzoate.

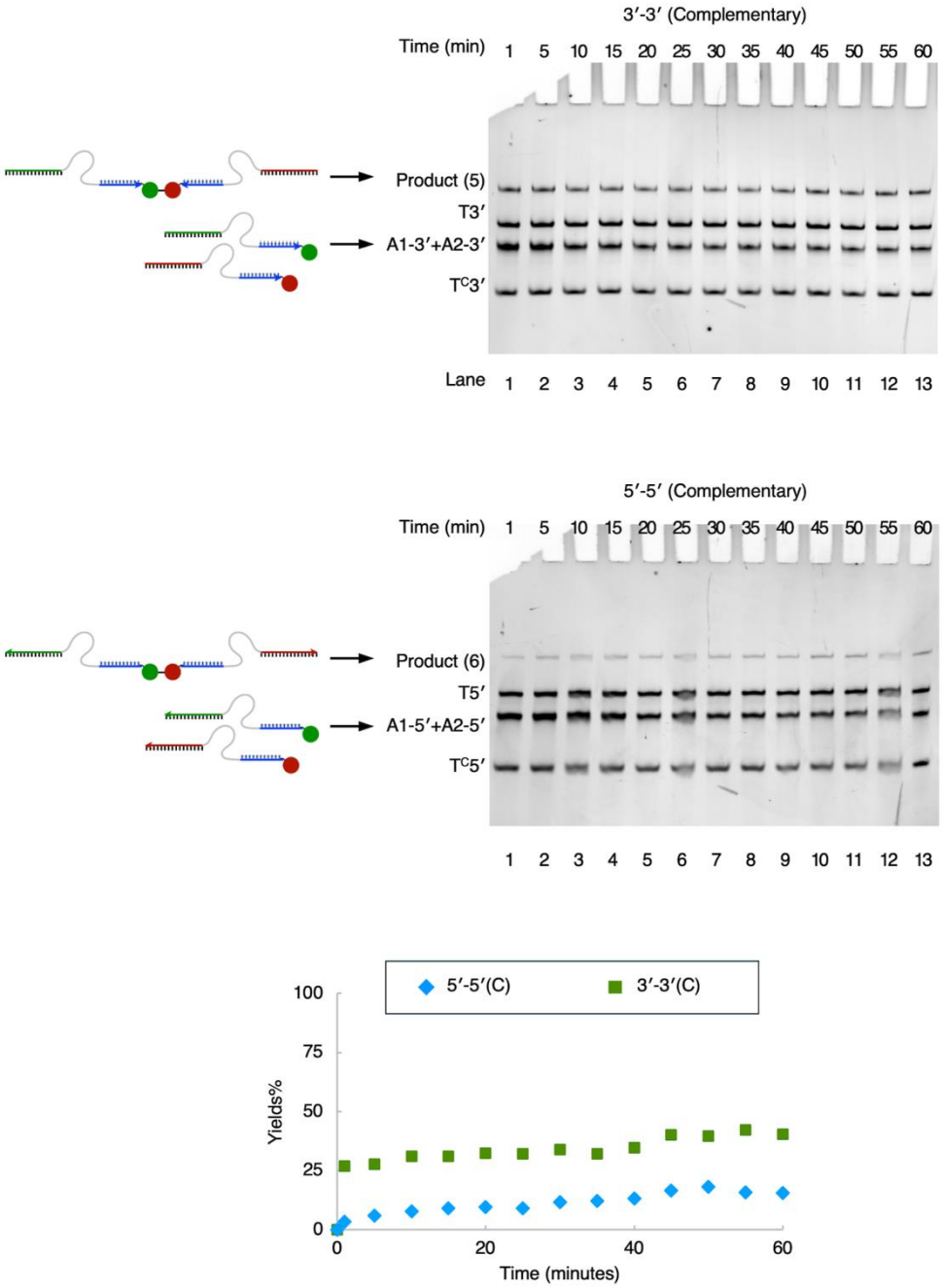

3.8. Figure S8. Denaturing PAGE analysis of DNA-templated thiazolidine synthesis.

Templated thiazolidine synthesis between 3′-conjugated reactants is faster than between 5′-conjugated reactants. For more details, see "2.8. DNA-Templated Thiazolidine Synthesis" in the methods section. Sequences used in this experiment are: (For 3′-3′) T3′, T^C3′, A1-3′-Benzaldehyde, and A2-3′-Cysteine. (For 5′-5′) T5′, T^C5′, A1-5′-Benzaldehyde and A2-5′-Cysteine.

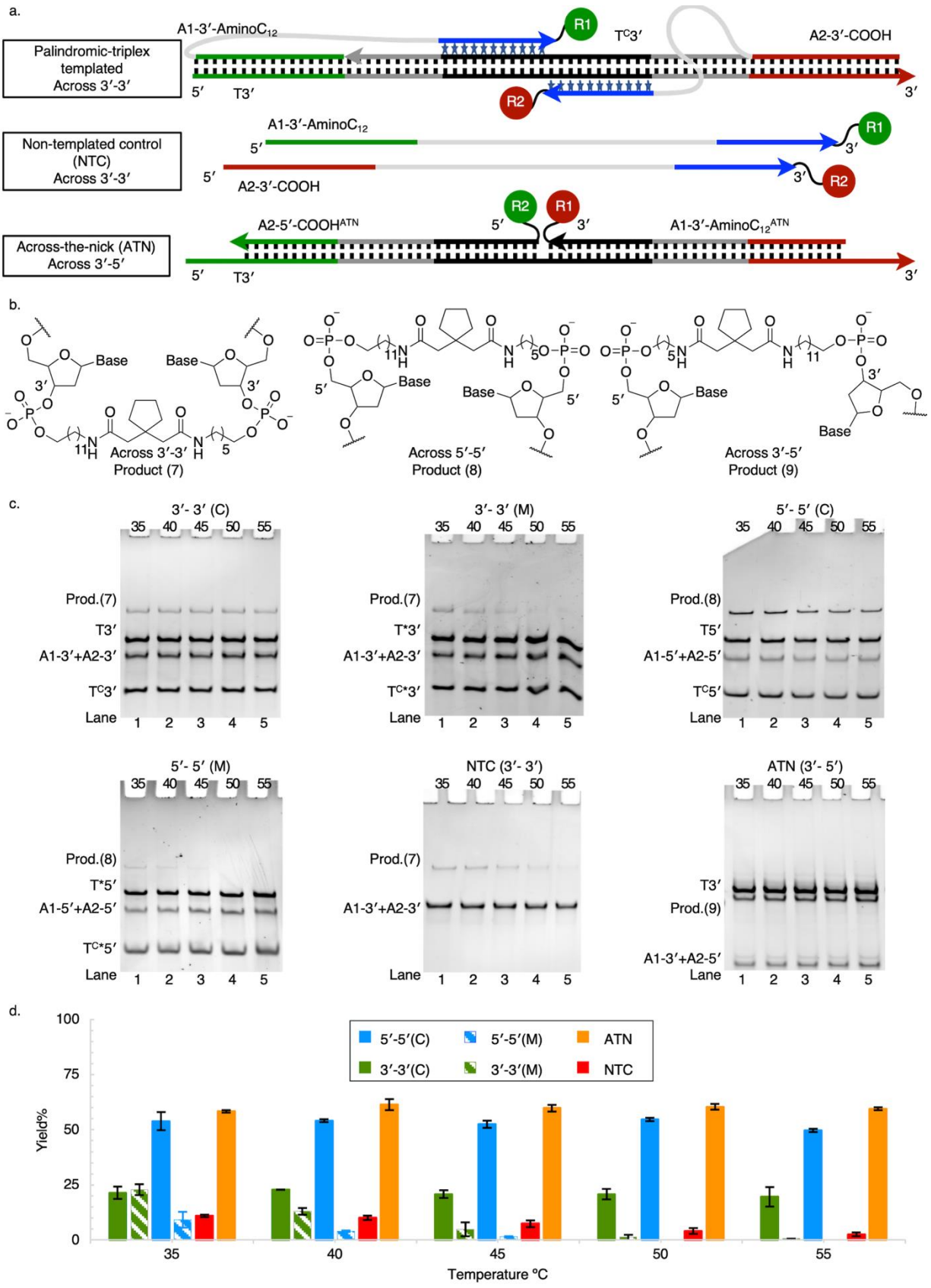

3.9. Figure S9. Denaturing PAGE analysis of DNA-templated amide-bond formation at different temperatures.

(a) Schematic representation of the triplex architecture for DNA-templated synthesis (C) with across-the-nick (ATN) and non-templated (NTC) controls. Base sequences of controls with mismatched triplex-forming domains (M) are

given in Figures 1, S2. Templated 3′-3′ and 5′-5′ reactions were as shown in Figure 2, although the linker to the amine reactive group in all reactions shown here contained a longer C_{12} chain (Figure S6). (b) Structures of products of DNA-templated conjugation. (c) Denaturing PAGE analysis of reaction products. (d) Reaction yields data are the average of two or three repeats conducted at each temperature. Error bars represent standard deviation for two or three repeats at each temperature. For more details, see "2.9. DNA-Templated Amide-Bond Formation at Different Temperatures" in the methods section. Sequences used in this experiment are: (For 3′-3′) T3′, T*3′, T^C3′, T^C*3′, A1-3′-AminoC_{12}, and A2-3′-COOH. (For 5′-5′) T5′, T*5′, T^C5′, T^C*5′, A1-5′-AminoC_{12}, and A2-5′-COOH. (For 3′-5′) T3′, A1-3′- AminoC_{12}^{ATN}, and A1-5′- $COOH^{ATN}$. (For NTC) A1-3′-AminoC_{12}, and A2-3′-COOH.

a.

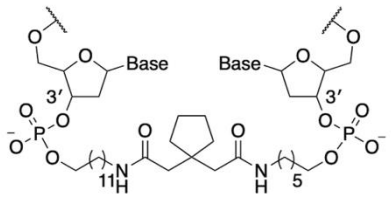

Across 3′-3′
Product (7)

b.

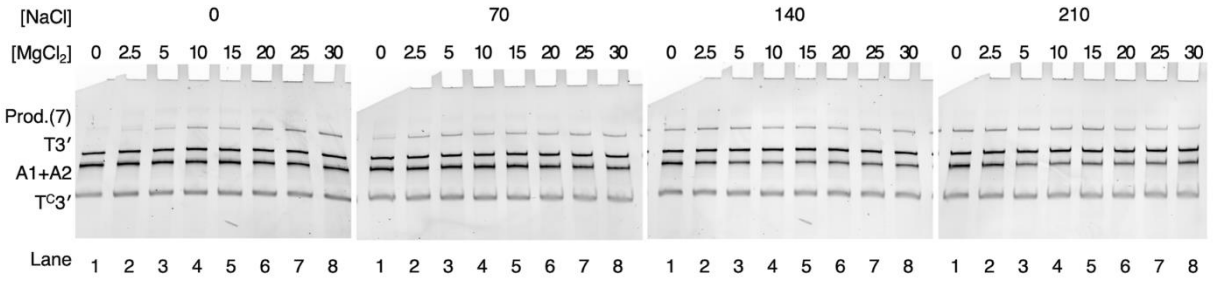

c.

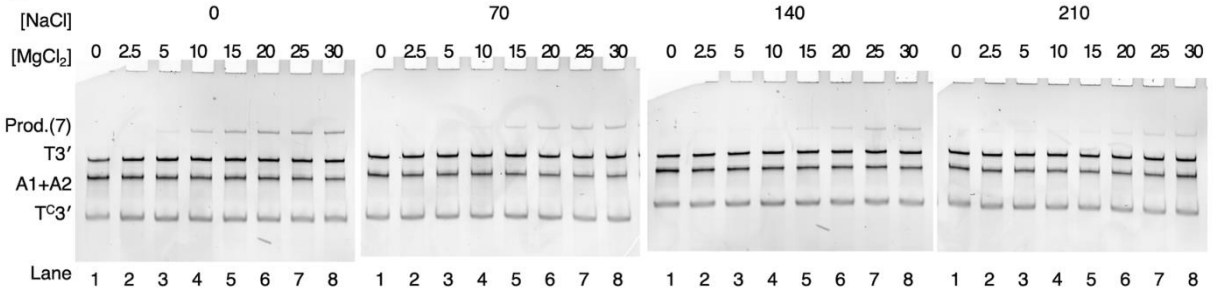

d.

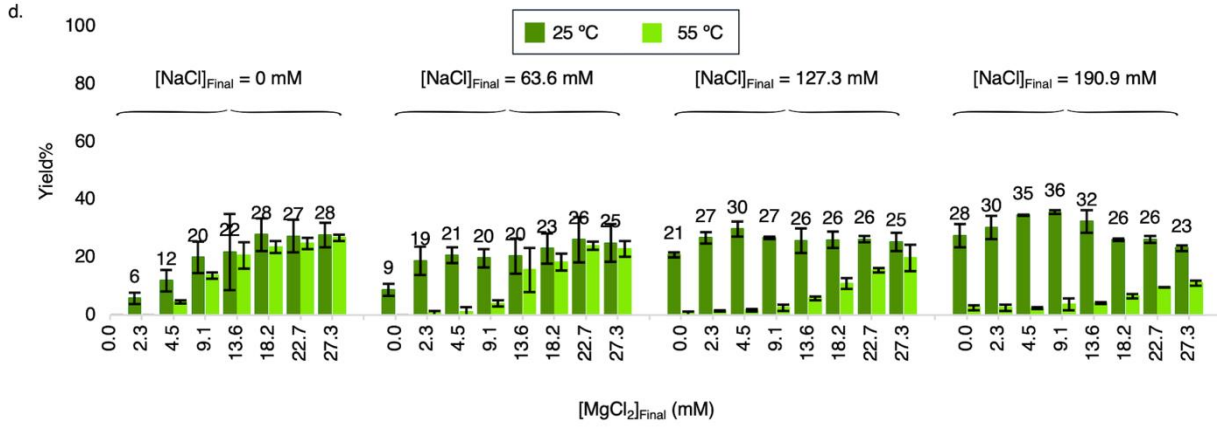

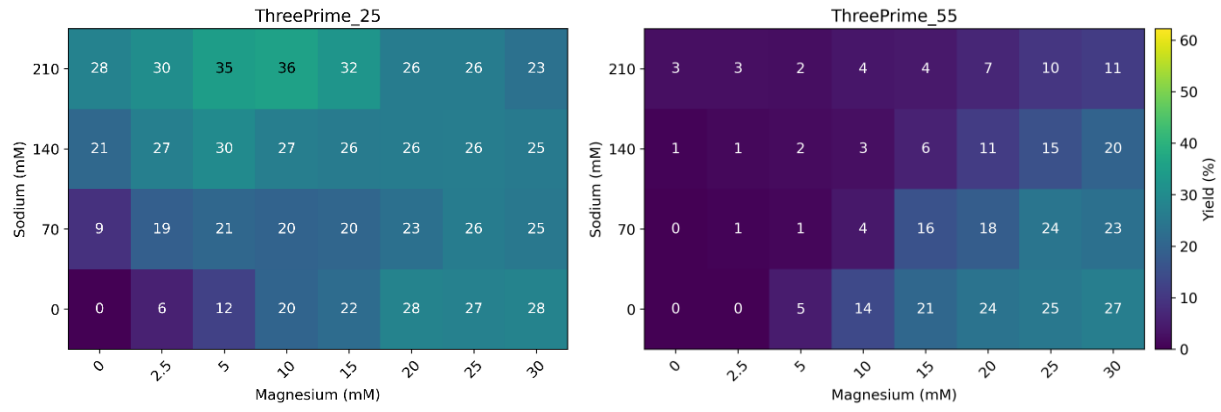

3.10. Figure S10. Denaturing PAGE analysis of DNA-templated amide-bond formation across 3′ ends under different salt conditions.

(a) Structure of DNA-encoded amide product (7) synthesised using reagents A1-3′-AminoC_{12} and A2-3′-COOH. (b) Denaturing PAGE analysis of DNA-templated amide-bond formation at 25 ºC. (c) Denaturing PAGE analysis of DNA-templated amide-bond formation at 55 ºC. (d) Histograms and heat maps showing the effect of cation concentration on DNA-templated amide-bond formation yields. For more details, see "2.10. DNA-Templated Amide-Bond Formation with Different Salt Concentrations" in the methods section. Sequences used in this experiment are for complementary 3′-3′: T3′, T^C3′, A1-3′-AminoC_{12}, and A2-3′-COOH.

a.

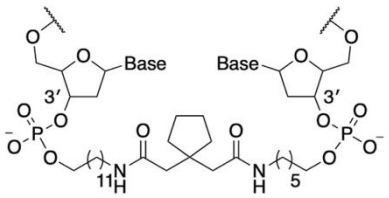

Across 3′-3′
Product (7)

b.

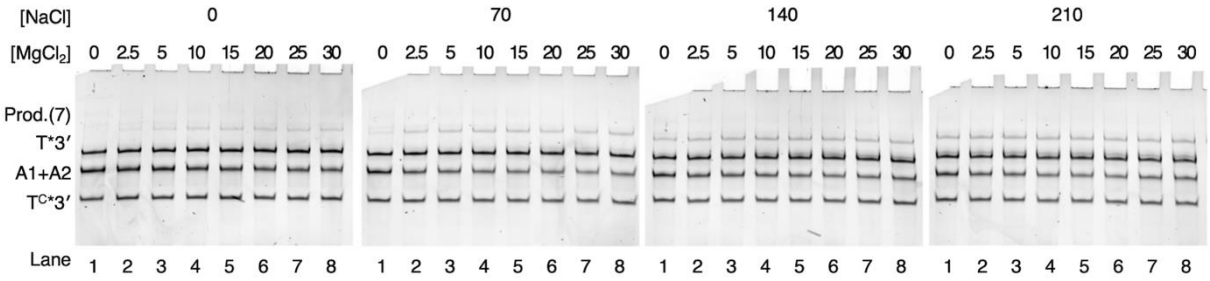

c.

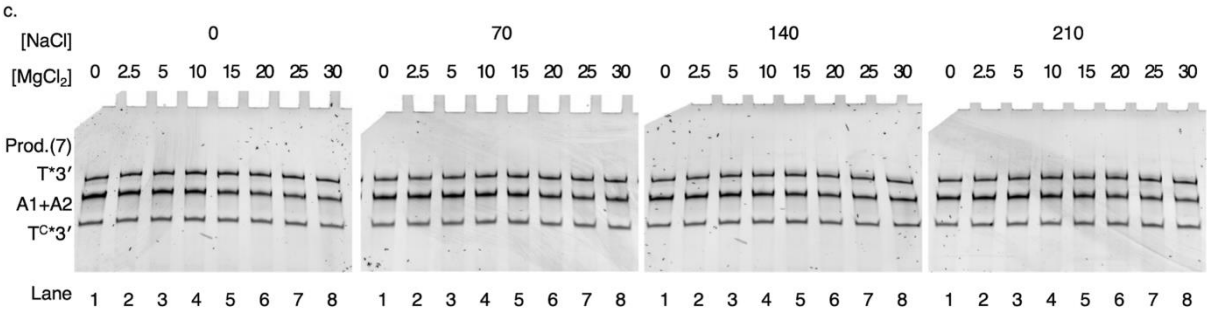

d.

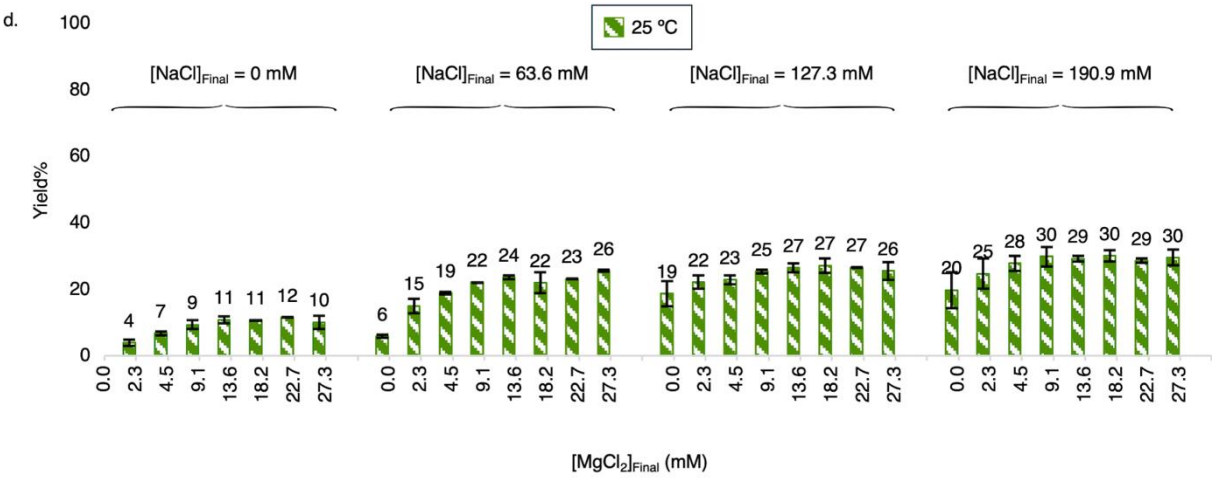

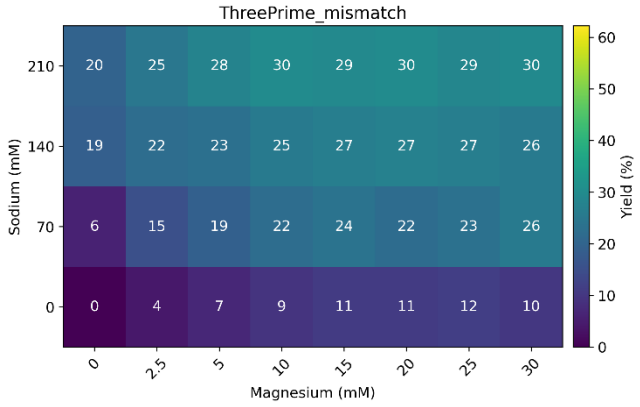

3.11. Figure S11. Denaturing PAGE analysis of DNA-templated amide-bond formation across 3′ ends under different salt conditions with mismatched triplex-forming domain.

(a) Structure of DNA-encoded amide product (7) synthesised using reagents A1-3′-AminoC_{12} and A2-3′-COOH. (b) Denaturing PAGE analysis of DNA-templated amide-bond formation at 25 ºC. (c) Denaturing PAGE analysis of DNA-templated amide-bond formation at 55 ºC. (d) Histogram and heat map showing the effect of cation concentration on DNA-templated amide-bond formation yields. For more details, see "2.10. DNA-Templated Amide-Bond Formation with Different Salt Concentrations" in the methods section. Sequences used in this experiment are for mismatched 3′-3′: T*3′, T^{C}*3′ (cf. Figure 1), A1-3′-AminoC_{12}, and A2-3′-COOH.

a.

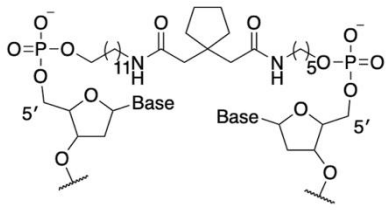

Across 5′-5′
Product (8)

b.

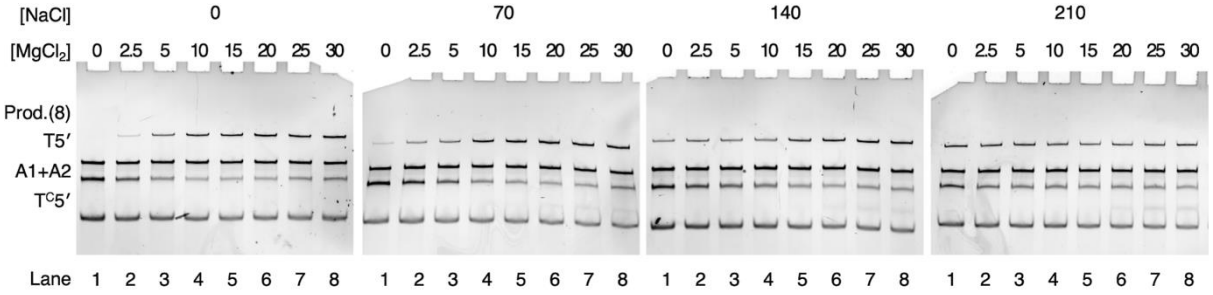

c.

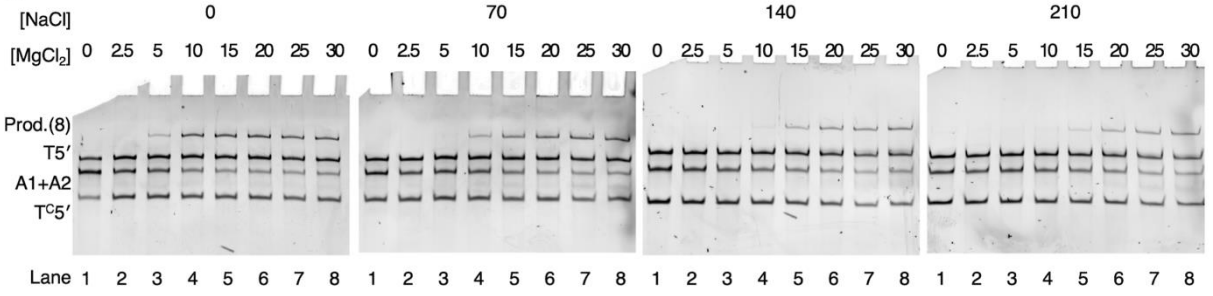

d.

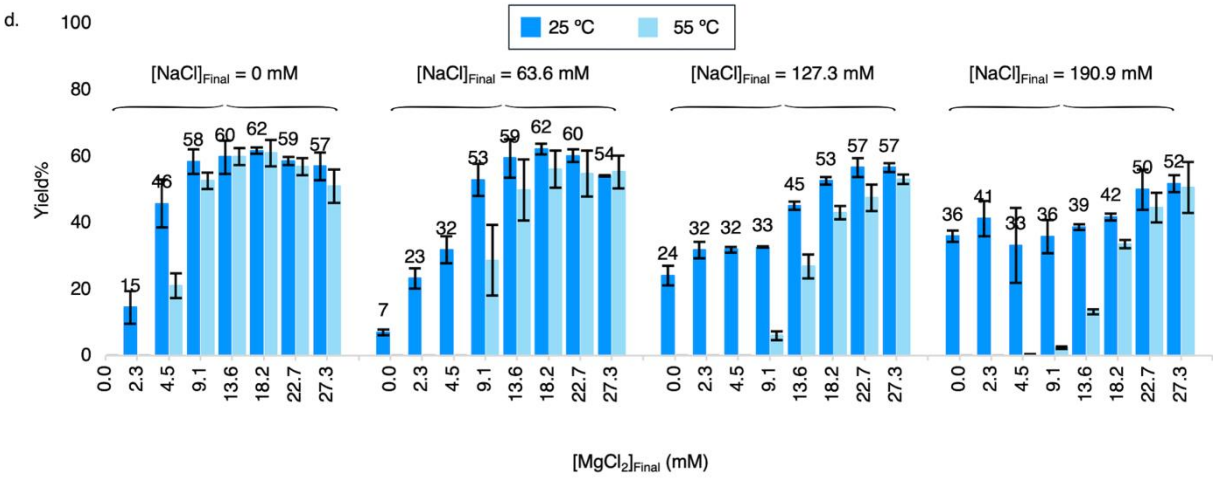

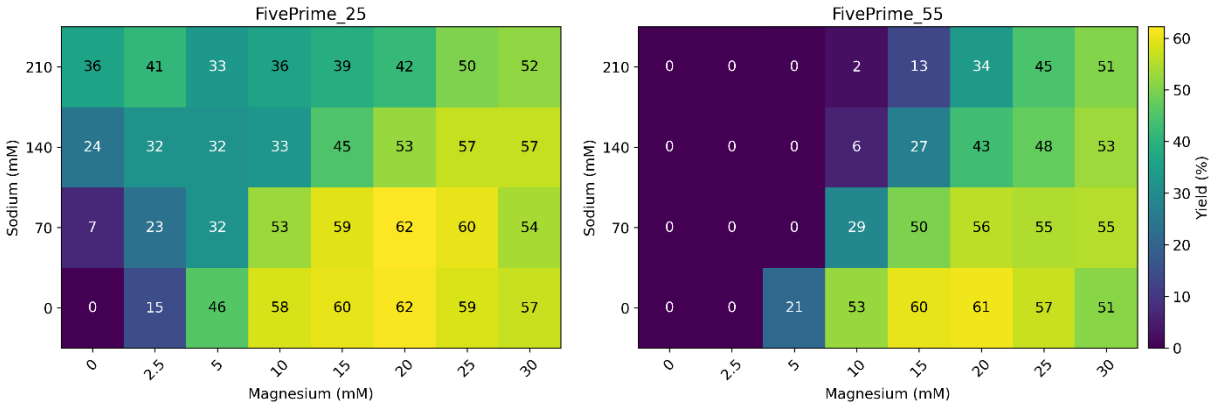

3.12. Figure S12. Denaturing PAGE analysis of DNA-templated amide-bond formation across 5′ ends under different salt conditions.

(a) Structure of DNA-encoded amide product (8) synthesised using reagents A1-5′-AminoC_{12} and A2-5′-COOH. (b) Denaturing PAGE analysis of DNA-templated amide-bond formation at 25 ºC. (c) Denaturing PAGE analysis of DNA-templated amide-bond formation at 55 ºC. (d) Histograms and heat maps showing the effect of cation concentration on DNA-templated amide-bond formation yields. For more details, see "2.10. DNA-Templated Amide-Bond Formation with Different Salt Concentrations" in the methods section. Sequences used in this experiment are for complementary 5′-5′: T5′, T^{C}5′, A1-5′-AminoC_{12}, and A2-5′-COOH.

a.

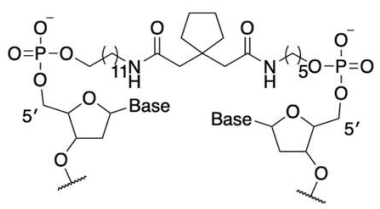

Across 5′-5′
Product (8)

b.

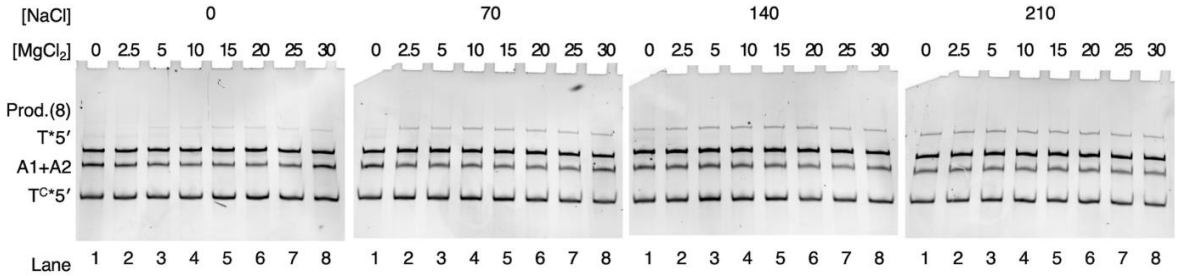

c.

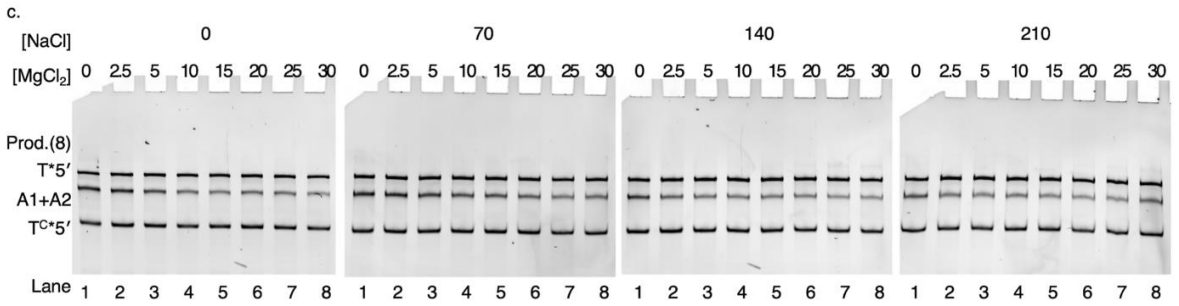

d.

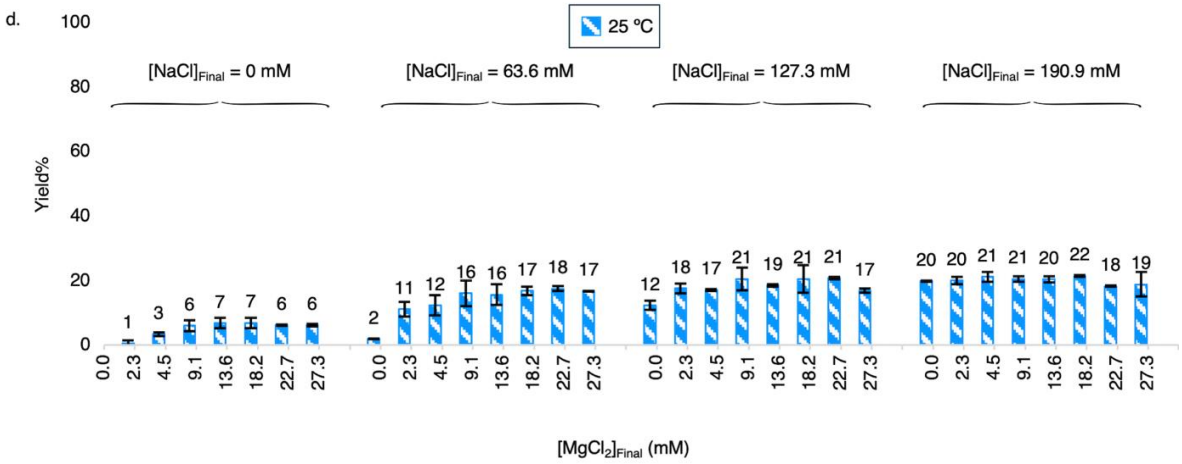

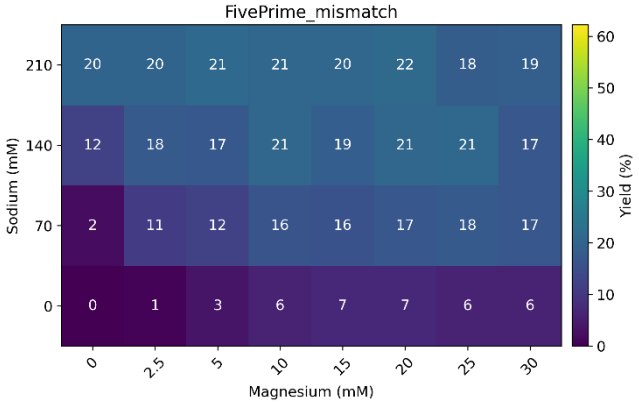

3.13. Figure S13. Denaturing PAGE analysis of DNA-templated amide-bond formation across 5′ ends under different salt conditions with mismatched triplex-forming domain.

(a) Structure of DNA-encoded amide product (8) synthesised using reagents A1-5′-AminoC_{12} and A2-5′-COOH. (b) Denaturing PAGE analysis of DNA-templated amide-bond formation at 25 ºC. (c) Denaturing PAGE analysis of DNA-templated amide-bond formation at 55 ºC. (d) Histogram and heat map showing the effect of cation concentration on DNA-templated amide-bond formation yields. (There was no observable reaction yield at 55 ºC.). For more details, see "2.10. DNA-Templated Amide-Bond Formation with Different Salt Concentrations" in the methods section. Sequences used in this experiment are for mismatched 5′-5′: T*5′, T^{C}*5′ (cf. Figure S2), A1-5′-AminoC_{12}, and A2-5′-COOH.

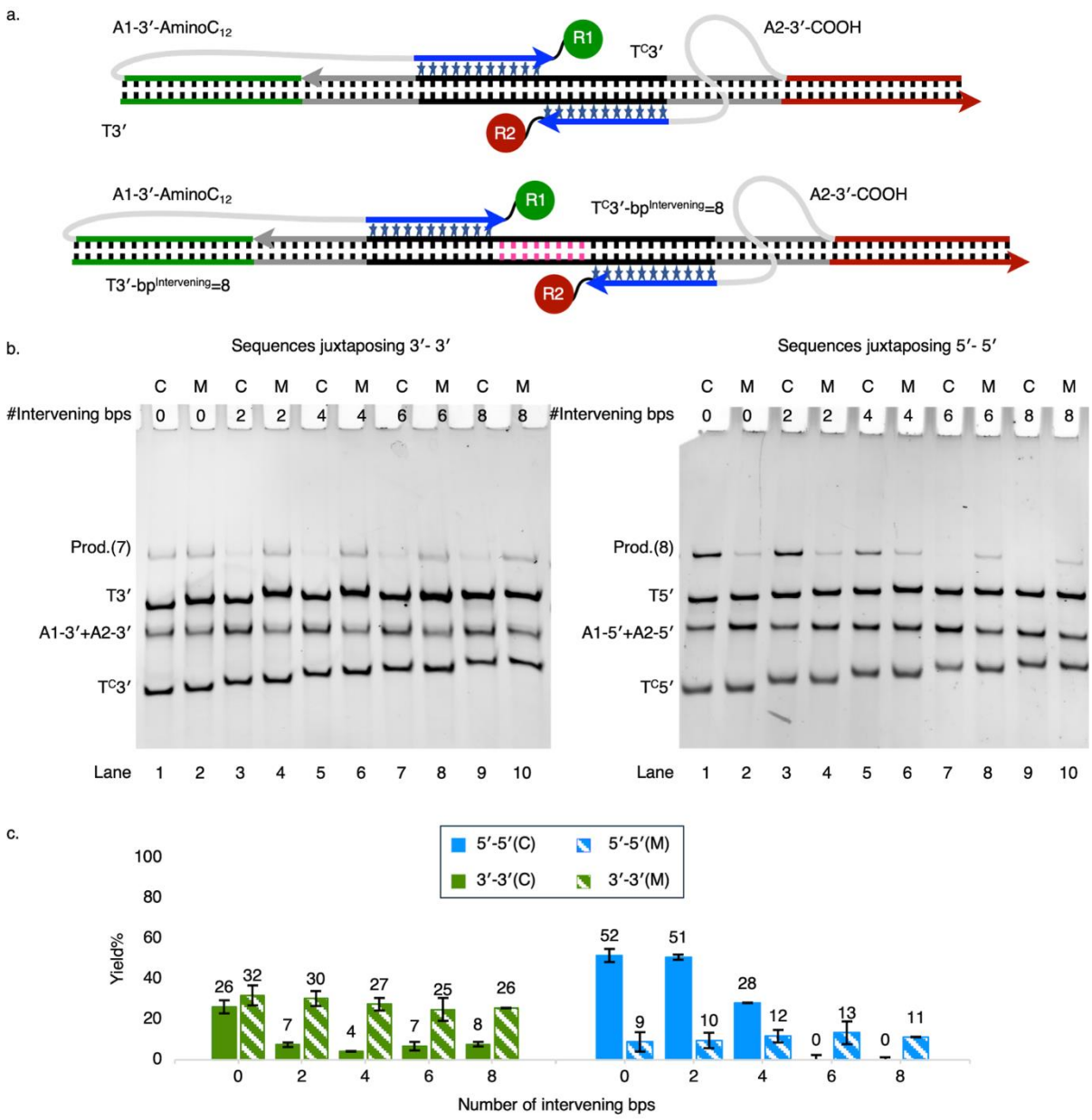

3.14. Figure S14. Analysis by denaturing PAGE of effect of intervening base pairs on DNA-templated amide-bond formation.

(a) Schematic representation of complexes juxtaposing like ends (3′-3′) through triple-helix formation with 0 (top) and 8 (bottom) intervening bps. (b) Denaturing PAGE analysis of DNA-templated amide-bond formation encoded by templates with complementary (C) and mismatched (M) triplex-forming domains (cf. Figure 1, Figure S2) with different numbers of bps between triplex domains. (c) Histograms showing a significant reduction in coupling yields with increasing number of intervening bps when reaction is templated using the triplex-complementary sequences. Yield using triplex-mismatched sequences is less sensitive to intervening base pairs. For more details, see "2.11. Effect of intervening base pairs on DNA-Templated Amide-Bond Formation" in the methods section. Sequences used for 3′-3′: T3′, T*3′, T^{C}3′, T^{C}*3′, T3′-$bp^{Intervening}$ =2-8, T^{C}3′-$bp^{Intervening}$=2-8, T*3′-$bp^{Intervening}$=2-8, T^{C}*3′-$bp^{Intervening}$=2-8, A1-3′-$AminoC_{12}$, and A2-3′-COOH, and for 5′-5′: T5′, T*5′, T^{C}5′, T^{C}*5′, T5′-$bp^{Intervening}$=2-8, TC5′-$bp^{Intervening}$=2-8, T*5′-$bp^{Intervening}$=2-8, T^{C}*5′-$bp^{Intervening}$=2-8, A1-5′-$AminoC_{12}$, and A2-5′-COOH.

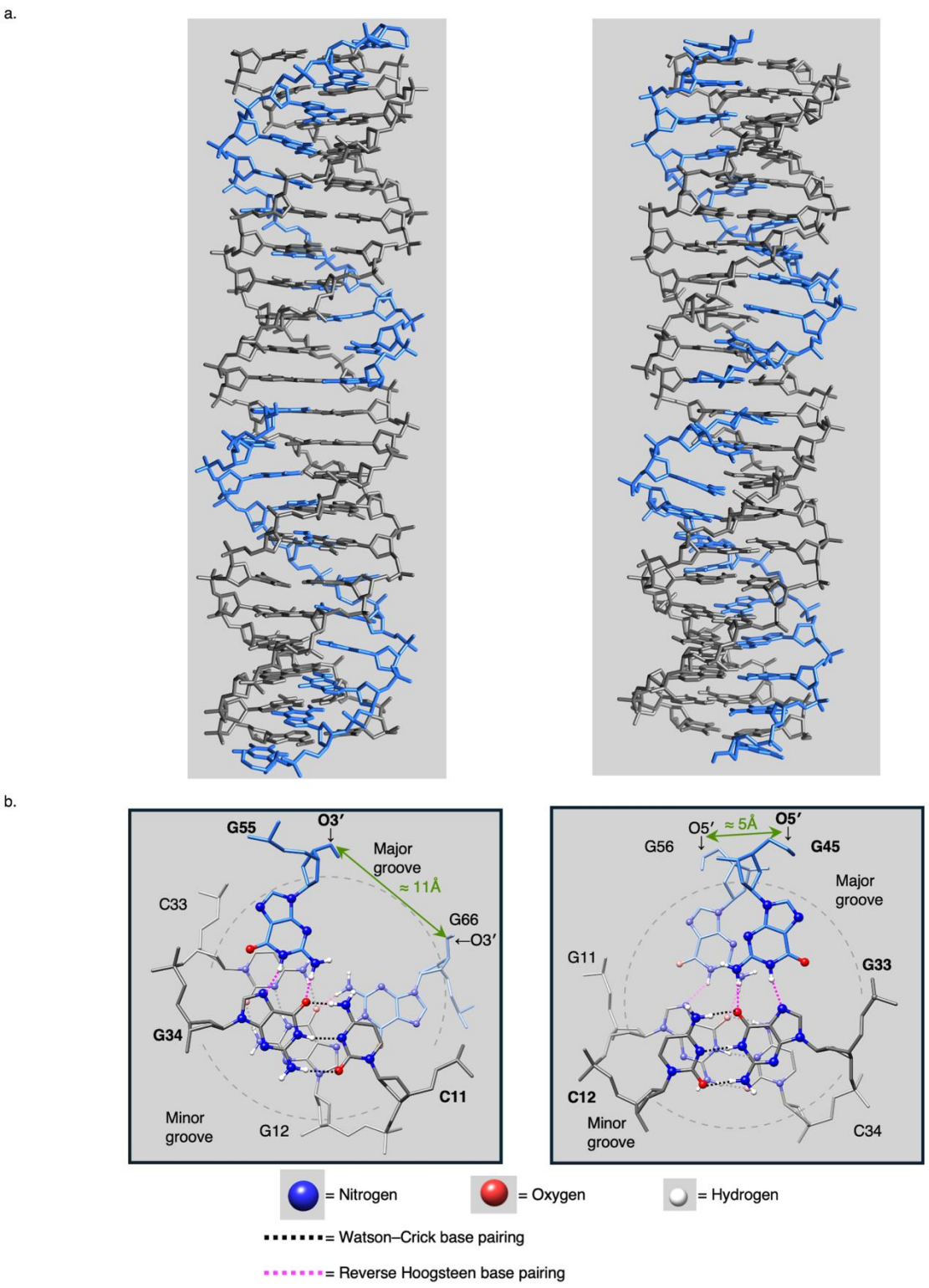

3.15. Figure S15. 3D models of the palindromic DNA triplex juxtaposing like ends.

(a) Structures of the triplexes juxtaposing 3′ ends (left) and 5′ ends (right). (b) Stacking of the base triplets on either side of the junctions that juxtapose 3′ ends (left) and 5′ ends (right). The sugar moieties, to which reactive linkers are attached, are closer together across the 5′-5′ junction.

4. Supporting Spectra

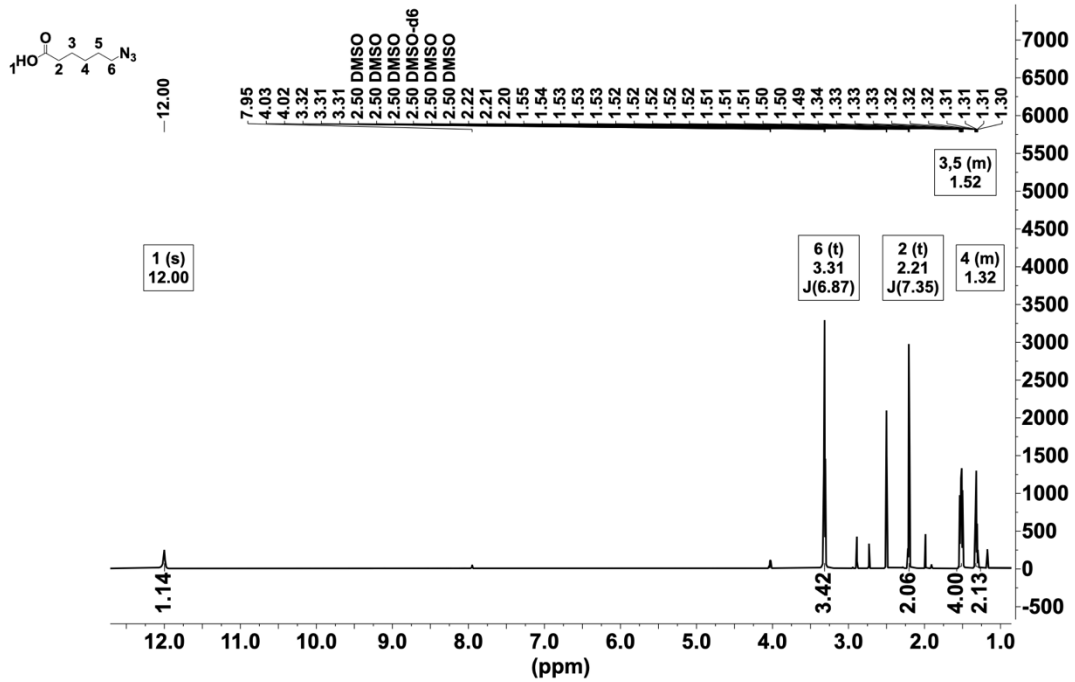

4.1. Supporting spectrum S1.

^{1}H NMR spectrum of 6-azidohexanoic acid (750 MHz, DMSO-d6, 298 K).

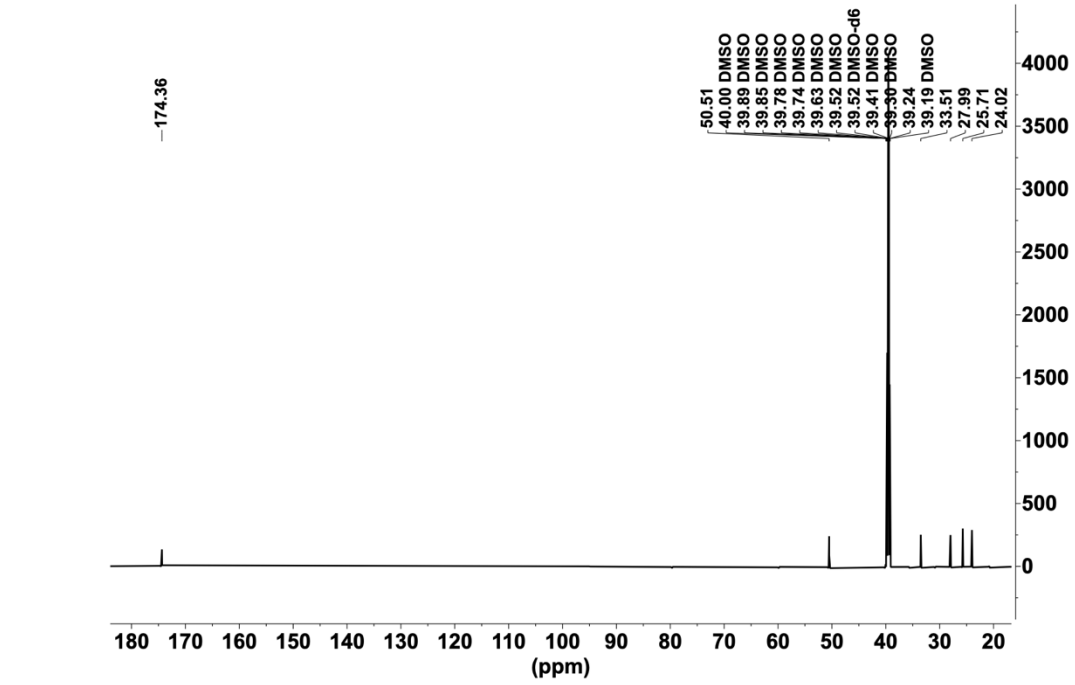

4.2. Supporting spectrum S2.

^{13}C NMR spectrum of 6-azidohexanoic acid (189 MHz, DMSO-d6, 298 K).

5. DNA Sequences and Modifications

All ssDNA sequences are written 5′ … 3′.

5.1. Complementary T And T^C for Complexes Juxtaposing 3′-3′

T3′	CGA GCG AGC CGA CAC GCG TTG TCG CGT CCC CTC CCT CGA GGG AGG GGA TGA GCC AAG CCG CAC AGT GGG ACC GC
T3′- $bp^{Intervening}$ =2	CGA GCG AGC CGA CAC GCG TTG TCG CGT CCC CTC CCT CTT GAG GGA GGG GAT GAG CCA AGC CGC ACA GTG GGA CCG C
T3′- $bp^{Intervening}$ =4	CGA GCG AGC CGA CAC GCG TTG TCG CGT CCC CTC CCT CTT TTG AGG GAG GGG ATG AGC CAA GCC GCA CAG TGG GAC CGC
T3′- $bp^{Intervening}$ =6	CGA GCG AGC CGA CAC GCG TTG TCG CGT CCC CTC CCT CTT TTT TGA GGG AGG GGA TGA GCC AAG CCG CAC AGT GGG ACC GC
T3′- $bp^{Intervening}$ =8	CGA GCG AGC CGA CAC GCG TTG TCG CGT CCC CTC CCT CTT TTT TTT GAG GGA GGG GAT GAG CCA AGC CGC ACA GTG GGA CCG C
T^C3′	GCT TGG CTC ATC CCC TCC CTC GAG GGA GGG GAC GCG ACA ACG
T^C3′-$bp^{Intervening}$ =2	GCT TGG CTC ATC CCC TCC CTC AAG AGG GAG GGG ACG CGA CAA CG
T^C3′-$bp^{Intervening}$ =4	GCT TGG CTC ATC CCC TCC CTC AAA AGA GGG AGG GGA CGC GAC AAC G
T^C3′-$bp^{Intervening}$ =6	GCT TGG CTC ATC CCC TCC CTC AAA AAA GAG GGA GGG GAC GCG ACA ACG
T^C3′-$bp^{Intervening}$ =8	GCT TGG CTC ATC CCC TCC CTC AAA AAA AAG AGG GAG GGG ACG CGA CAA CG

5.2. Mismatched T* And T^{C}* for Complexes Juxtaposing 3′-3′

T*3′	CGA GCG AGC CGA CAC GCG TTG TCG CGT GGG GTG GCT CGA GCC ACC CCA TGA GCC AAG CCG CAC AGT GGG ACC GC
T*3′- $bp^{Intervening}$ =2	CGA GCG AGC CGA CAC GCG TTG TCG CGT GGG GTG GCT CTT GAG CCA CCC CAT GAG CCA AGC CGC ACA GTG GGA CCG C
T*3′- $bp^{Intervening}$ =4	CGA GCG AGC CGA CAC GCG TTG TCG CGT GGG GTG GCT CTT TTG AGC CAC CCC ATG AGC CAA GCC GCA CAG TGG GAC CGC
T*3′- $bp^{Intervening}$ =6	CGA GCG AGC CGA CAC GCG TTG TCG CGT GGG GTG GCT CTT TTT TGA GCC ACC CCA TGA GCC AAG CCG CAC AGT GGG ACC GC
T*3′- $bp^{Intervening}$ =8	CGA GCG AGC CGA CAC GCG TTG TCG CGT GGG GTG GCT CTT TTT TTT GAG CCA CCC CAT GAG CCA AGC CGC ACA GTG GGA CCG C
T^{C}*3′	GCT TGG CTC ATG GGG TGG CTC GAG CCA CCC CAC GCG ACA ACG
T^{C}*3′- $bp^{Intervening}$ =2	GCT TGG CTC ATG GGG TGG CTC AAG AGC CAC CCC ACG CGA CAA CG
T^{C}*3′- $bp^{Intervening}$ =4	GCT TGG CTC ATG GGG TGG CTC AAA AGA GCC ACC CCA CGC GAC AAC G
T^{C}*3′- $bp^{Intervening}$ =6	GCT TGG CTC ATG GGG TGG CTC AAA AAA GAG CCA CCC CAC GCG ACA ACG
T^{C}*3′- $bp^{Intervening}$ =8	GCT TGG CTC ATG GGG TGG CTC AAA AAA AAG AGC CAC CCC ACG CGA CAA CG

5.3. Adapters A_1 And A_2 for Complexes Juxtaposing 3′-3′

A1-3′	CGT GTC GGC TCG CTC GTT TTT TTT TTT TTT TTT TTT TTT TTT TTT TTT GGG GTG GGT G
A2-3′	GCG GTC CCA CTG TGC GTT TTT TTT TTT TTT TTT TTT TTT TTT TTT TTT GGG GTG GGT G
A1-3′-AminoC_{12}	CGT GTC GGC TCG CTC GTT TTT TTT TTT TTT TTT TTT TTT TTT TTT TTT GGG GTG GGT G/Aminolink C12/
A1-3′-AminoC_6	CGT GTC GGC TCG CTC GTT TTT TTT TTT TTT TTT TTT TTT TTT TTT TTT GGG GTG GGT G/Aminolink C6/
A2-3′-COOH	GCG GTC CCA CTG TGC GTT TTT TTT TTT TTT TTT TTT TTT TTT TTT TTT GGG GTG GGT G/COOH/
A1-3′-DBCO	CGT GTC GGC TCG CTC GTT TTT TTT TTT TTT TTT TTT TTT TTT TTT TTT GGG GTG GGT G/DBCO/

A2-3′-Azidobenzoate	GCG GTC CCA CTG TGC GTT TTT TTT TTT TTT TTT TTT TTT TTT TTT TTT GGG GTG GGT G/Azidobenzoate/
A1-3′-Benzaldehyde	CGT GTC GGC TCG CTC GTT TTT TTT TTT TTT TTT TTT TTT TTT TTT TTT GGG GTG GGT G/ Benzaldehyde /
A2-3′-Cysteine	GCG GTC CCA CTG TGC GTT TTT TTT TTT TTT TTT TTT TTT TTT TTT TTT GGG GTG GGT G/ Cysteine/
A1-3′-Cy3	CGT GTC GGC TCG CTC GTT TTT TTT TTT TTT TTT TTT TTT TTT TTT TTT GGG GTG GGT G/Cy3/
A2-3′-Cy5	GCG GTC CCA CTG TGC GTT TTT TTT TTT TTT TTT TTT TTT TTT TTT TTT GGG GTG GGT G/Cy5/

5.4. Complementary T And TC for Complexes Juxtaposing 5′-5′

T5′	CGC CAG GGT GAC ACG CCG AAC CGA GTA GGG GAG GGA GCT CCC TCC CCT GCG CTG TTG CGC ACA GCC GAG CGA GC
T5′- $bp^{Intervening}$ =2	CGC CAG GGT GAC ACG CCG AAC CGA GTA GGG GAG GGA GTT CTC CCT CCC CTG CGC TGT TGC GCA CAG CCG AGC GAG C
T5′- $bp^{Intervening}$ =4	CGC CAG GGT GAC ACG CCG AAC CGA GTA GGG GAG GGA GTT TTC TCC CTC CCC TGC GCT GTT GCG CAC AGC CGA GCG AGC
T5′- $bp^{Intervening}$ =6	CGC CAG GGT GAC ACG CCG AAC CGA GTA GGG GAG GGA GTT TTT TCT CCC TCC CCT GCG CTG TTG CGC ACA GCC GAG CGA GC
T5′- $bp^{Intervening}$ =8	CGC CAG GGT GAC ACG CCG AAC CGA GTA GGG GAG GGA GTT TTT TTT CTC CCT CCC CTG CGC TGT TGC GCA CAG CCG AGC GAG C
T^C5′	GCA ACA GCG CAG GGG AGG GAG CTC CCT CCC CTA CTC GGT TCG
T^C5′- $bp^{Intervening}$ =2	GCA ACA GCG CAG GGG AGG GAG AAC TCC CTC CCC TAC TCG GTT CG
T^C5′- $bp^{Intervening}$ =4	GCA ACA GCG CAG GGG AGG GAG AAA ACT CCC TCC CCT ACT CGG TTC G
T^C5′- $bp^{Intervening}$ =6	GCA ACA GCG CAG GGG AGG GAG AAA AAA CTC CCT CCC CTA CTC GGT TCG
T^C5′- $bp^{Intervening}$ =8	GCA ACA GCG CAG GGG AGG GAG AAA AAA AAC TCC CTC CCC TAC TCG GTT CG

5.5. Mismatched T* And T^{C}* for Complexes Juxtaposing 5′-5′

T*5′	CGC CAG GGT GAC ACG CCG AAC CGA GTA GGG GAG GGA GCT CCC TCC CCT GCG CTG TTG CGC ACA GCC GAG CGA GC
T*5′- $bp^{Intervening}$ =2	CGC CAG GGT GAC ACG CCG AAC CGA GTA CCC CAC CGA GTT CTC GGT GGG GTG CGC TGT TGC GCA CAG CCG AGC GAG C
T*5′- $bp^{Intervening}$ =4	CGC CAG GGT GAC ACG CCG AAC CGA GTA CCC CAC CGA GTT TTC TCG GTG GGG TGC GCT GTT GCG CAC AGC CGA GCG AGC
T*5′- $bp^{Intervening}$ =6	CGC CAG GGT GAC ACG CCG AAC CGA GTA CCC CAC CGA GTT TTT TCT CGG TGG GGT GCG CTG TTG CGC ACA GCC GAG CGA GC
T*5′- $bp^{Intervening}$ =8	CGC CAG GGT GAC ACG CCG AAC CGA GTA CCC CAC CGA GTT TTT TTT CTC GGT GGG GTG CGC TGT TGC GCA CAG CCG AGC GAG C
T^{C}*5′	GCA ACA GCG CAG GGG AGG GAG CTC CCT CCC CTA CTC GGT TCG
T^{C}*5′- $bp^{Intervening}$ =2	GCA ACA GCG CAC CCC ACC GAG AAC TCG GTG GGG TAC TCG GTT CG
T^{C}*5′- $bp^{Intervening}$ =4	GCA ACA GCG CAC CCC ACC GAG AAA ACT CGG TGG GGT ACT CGG TTC G
T^{C}*5′- $bp^{Intervening}$ =6	GCA ACA GCG CAC CCC ACC GAG AAA AAA CTC GGT GGG GTA CTC GGT TCG
T^{C}*5′- $bp^{Intervening}$ =8	GCA ACA GCG CAC CCC ACC GAG AAA AAA AAC TCG GTG GGG TAC TCG GTT CG

5.6. Adapters A_1 And A_2 for Complexes Juxtaposing 5′-5′

A1-5′	GTG GGT GGG GTT TTT TTT TTT TTT TTT TTT TTT TTT TTT TTT GCT CGC TCG GCT GTG C
A2-5′	GTG GGT GGG GTT TTT TTT TTT TTT TTT TTT TTT TTT TTT TTT GCG TGT CAC CCT GGC G
A1-5′-AminoC_{12}	/Aminolink C12/GTG GGT GGG GTT TTT TTT TTT TTT TTT TTT TTT TTT TTT TTT GCT CGC TCG GCT GTG C
A1-5′-AminoC_5	/Aminolink C5/GTG GGT GGG GTT TTT TTT TTT TTT TTT TTT TTT TTT TTT TTT GCT CGC TCG GCT GTG C
A2-5′-COOH	/COOH/GTG GGT GGG GTT TTT TTT TTT TTT TTT TTT TTT TTT TTT TTT GCG TGT CAC CCT GGC G
A1-5′-DBCO	/DBCO/GTG GGT GGG GTT TTT TTT TTT TTT TTT TTT TTT TTT TTT TTT GCT CGC TCG GCT GTG C

A2-5′-Azidobenzoate	/Azidobenzoate/GTG GGT GGG GTT TTT TTT TTT TTT TTT TTT TTT TTT TTT TTT GCG TGT CAC CCT GGC G
A1-5′-Benzaldehyde	/Benzaldehyde /GTG GGT GGG GTT TTT TTT TTT TTT TTT TTT TTT TTT TTT TTT GCT CGC TCG GCT GTG C
A2-5′-Cysteine	/Cysteine/GTG GGT GGG GTT TTT TTT TTT TTT TTT TTT TTT TTT TTT TTT GCG TGT CAC CCT GGC G
A1-5′-Cy3	/Cy3/GTG GGT GGG GTT TTT TTT TTT TTT TTT TTT TTT TTT TTT TTT GCT CGC TCG GCT GTG C
A2-5′-Cy5	/Cy5/ GTG GGT GGG GTT TTT TTT TTT TTT TTT TTT TTT TTT TTT TTT GCG TGT CAC CCT GGC G

5.7. Complementary T for Complexes Juxtaposing 3′-5′

T3′	CGA GCG AGC CGA CAC GCG TTG TCG CGT CCC CTC CCT CGA GGG AGG GGA TGA GCC AAG CCG CAC AGT GGG ACC GC

5.8. Adapters A_1 And A_2 for Complexes Juxtaposing 3′-5′

A1-3′- $AminoC_{12}^{ATN}$	CCA CTG TGC GGC TTG GCT CAT CCC CTC CCT C/Aminolink C12/
A1-5′- $COOH^{ATN}$	/COOH/GAG GGA GGG GAC GCG ACA ACG CGT GTC GGC T

6. Supporting References

[36] L. J. Maher, P. B. Dervan, B. J. Wold, "Kinetic Analysis of Oligodeoxyribonucleotide-Directed Triple-Helix Formation on DNA" *Biochemistry (Easton)* **1990**, *29*, 8820-8826.

[37] B. Saccà, R. Meyer, U. Feldkamp, H. Schroeder, C. M. Niemeyer, "High-Throughput, Real-Time Monitoring of the Self-Assembly of DNA Nanostructures by FRET Spectroscopy" *Angew. Chem., Int. Ed.* **2008**, *47*, 2135-2137.

[38] B. Saccà, C. M. Niemeyer, R. Meyer, "Temperature-Dependent FRET Spectroscopy for the High-Throughput Analysis of Self-Assembled DNA Nanostructures in Real Time" *Nat. Protoc.* **2009**, *4*, 271-285.

[39] Y. You, A. V. Tataurov, R. Owczarzy, "Measuring thermodynamic details of DNA hybridization using fluorescence" *Biopolymers* **2011**, *95*, 472-486.

[40] T. Kekić, J. Lietard, "Sequence-dependence of Cy3 and Cy5 dyes in 3′ terminally-labeled single-stranded DNA" *Sci. Rep.* **2022**, *12*, 14803-14809.

[41] Y. Liu, D. M. J. Lilley, "Crystal Structures of Cyanine Fluorophores Stacked onto the End of Double-Stranded RNA" *Biophys. J.* **2017**, *113*, 2336-2343.

[42] A. Iqbal, L. Wang, K. C. Thompson, D. M. J. Lilley, D. G. Norman, "The Structure of Cyanine 5 Terminally Attached to Double-Stranded DNA: Implications for FRET Studies" *Biochemistry* **2008**, *47*, 7857-7862.

[43] S. Ohkuma, B. Poole, "Fluorescence Probe Measurement of the Intralysosomal pH in Living Cells and the Perturbation of pH by Various Agents" *Proc. Natl. Acad. Sci. U. S. A.* **1978**, *75*, 3327-3331.

[44] N. DiCesare, J. R. Lakowicz, "Spectral Properties of Fluorophores Combining the Boronic Acid Group with Electron Donor or Withdrawing Groups. Implication in the Development of Fluorescence Probes for Saccharides" *J. Phys. Chem. A.* **2001**, *105*, 6834-6840.

[45] Z. Murtaza, Q. Chang, G. Rao, H. Lin, J. R. Lakowicz, "Long-Lifetime Metal–Ligand pH Probe" *Anal. Biochem.* **1997**, *247*, 216-222.

[46] J. L. Mergny, L. Lacroix, "UV Melting of G-Quadruplexes" *Curr. Protoc. Nucleic Acid Chem.* **2009**, *37*, 17.11.11-17.11.15.

[47] A. Mariani, A. Bartoli, M. Atwal, K. C. Lee, C. A. Austin, R. l. Rodriguez, "Differential Targeting of Human Topoisomerase II Isoforms with Small Molecules" *J. Med. Chem.* **2015**, *58*, 4851-4856.

[48] B. C. Froehler, T. Terhorst, J. P. Shaw, S. N. McCurdy, "Triple-helix formation and cooperative binding by oligodeoxynucleotides with a 3'-3' internucleotide junction" *Biochemistry (Easton)* **1992**, *31*, 1603-1609.

[49] Maestro Version 12.9.123, MMshare Version 5.5.123, Release 2021-3. Schrödinger LLC, New York.

[50] L. P. P. Patro, A. Kumar, N. Kolimi, T. Rathinavelan, "3D-NuS: A Web Server for Automated Modeling and Visualization of Non-Canonical 3-Dimensional Nucleic Acid Structures" *J. Mol. Biol.* **2017**, *429*, 2438-2448.

[51] H. J. C. Berendsen, D. van der Spoel, R. van Drunen, "GROMACS: A message-passing parallel molecular dynamics implementation" *Comput. Phys. Commun.* **1995**, *91*, 43-56.

[52] N. Foloppe, J. A. D. MacKerell, "All-atom empirical force field for nucleic acids: I. Parameter optimization based on small molecule and condensed phase macromolecular target data" *J. Comput. Chem.* **2000**, *21*, 86-104.

[53] A. D. MacKerell, N. K. Banavali, "All-atom empirical force field for nucleic acids: II. Application to molecular dynamics simulations of DNA and RNA in solution" *J. Comput. Chem.* **2000**, *21*, 105-120.

[54] P. r. Bjelkmar, P. Larsson, M. A. Cuendet, B. Hess, E. Lindahl, "Implementation of the CHARMM Force Field in GROMACS: Analysis of Protein Stability Effects from Correction Maps, Virtual Interaction Sites, and Water Models" *J. Chem. Theory Comput.* **2010**, *6*, 459-466.

[55] E. F. Pettersen, T. D. Goddard, C. C. Huang, G. S. Couch, D. M. Greenblatt, E. C. Meng, T. E. Ferrin, "UCSF Chimera-A visualization system for exploratory research and analysis" *J. Comput. Chem.* **2004**, *25*, 1605-1612.